PHILOSOPHICAL TRANSACTIONS OF THE ROYAL SOCIETY A MATHEMATICAL, PHYSICAL & ENGINEERING SCIENCES

On the Praseodymium+Oxygen System

B. G. Hyde, D. J. M. Bevan and L. Eyring

Phil. Trans. R. Soc. Lond. A 1966 **259**, 583-614
doi: 10.1098/rsta.1966.0025

ON THE PRASEODYMIUM+OXYGEN SYSTEM

BY B. G. HYDE,† D. J. M. BEVAN‡ AND L. EYRING
Chemistry Department, Arizona State University, Tempe, Arizona, U.S.A.

(*Communicated by J. S. Anderson, F.R.S.—Received* 12 *November* 1964—
Revised 26 *August* 1965)

[Plate 11]

CONTENTS

An isobaric survey of the system praseodymium oxide+oxygen has been made at oxygen pressures between 0 and 1 atm and in the temperature range 200 to 1150 °C. The derived isobaric sections enable a three-dimensional phase diagram (pressure, temperature, composition) to be constructed with considerable certainty and detail for the composition range $PrO_{1\cdot65}$ to $PrO_{1\cdot84}$. Reasonable extensions to cover the complete range between the sesquioxide and dioxide are proposed, and a projection of the diagram on to the temperature-composition plane is presented. At lower temperatures several discrete, ordered phases of narrow homogeneity range exist. These constitute an homologous series Pr_nO_{2n-2}, with $n = 4, 7, 9, 10, 11, 12, \infty$. At higher temperatures two wide-range solid solutions obtain: σ, a body-centred cubic phase with a maximum composition range *ca.* $PrO_{1\cdot60}$ to $PrO_{1\cdot70}$; and α, a face-centred cubic phase of composition *ca.* $PrO_{1\cdot72}$ to PrO_2. The fields of stability of the various phases are defined and the ambient conditions at many invariant axes (peritectoid and eutectoid) enumerated.

Miscibility gaps with upper consolute points are exceptional; order-disorder peritectoid transformations are common. Hysteresis in phase transformations is confirmed, and the results further demonstrate the existence of metastable states in phase reactions involving an increase in structural order. The appearance of these *pseudo-phases* and the nature of non-stoichiometry is explained in terms of a plausible model invoking microdomain texture in defect solids. This model is believed to be appropriate for other non-stoichiometric systems also.

Earlier experimental data on the system are examined, and found to be consistent with the present results.

† Present address, University of Western Australia, Nedlands, Western Australia.
‡ On leave from the University of Western Australia.

VOL. 259. A. 1106. (Price 13*s.* 6*d*; U.S. $2.00) 70 [Published 19 May 1966

1. Introduction

Over a number of years there has been a continuing interest in binary and ternary solid oxide systems in which non-stoichiometric phases, often of quite large compositional width, have been reported. These phases have usually been described in terms of the classical model of point defects randomly distributed on the lattice of a parent structure (Wagner & Schottky 1930; Anderson 1945). Recently, with more incisive techniques, the trend has been for extended compositional regions of supposed homogeneity to be resolved into a number of phases having unusual but precise stoichiometries and unique structures with no appreciable concentration of point defects. For a given system these structures are closely related to each other and to a simple parent structure (see, for example, Wadsley 1964). An example is provided by the titanium oxides, TiO_x, where two supposedly homogeneous regions ($1{\cdot}65 \leqslant x \leqslant 1{\cdot}80$; $1{\cdot}90 \leqslant x \leqslant 2{\cdot}00$) have been resolved into an homologous series of stoichiometric oxides Ti_nO_{2n-1} ($n = 4, 5, 6, 7, 8, 9, 10, \infty$) and intervening diphasic regions (Andersson, Collén, Kuylenstierna & Magnéli 1957; Andersson 1960). No compositional width was detectable by lattice parameter measurements. Similar behaviour has been observed in many other systems and one must conclude that, in these cases, the earlier evidence for gross non-stoichiometry is erroneous, either because there were too few data or because of lack of equilibrium in the system under examination, or both.

Consequently, there has developed a lack of confidence in the classical model of defect structures. As a result of the crystallographic findings in particular, one might justifiably consider the extreme point of view that, *at equilibrium*, non-stoichiometric phases, and particularly gross non-stoichiometry, do not exist. However, there is substantial experimental evidence indicating that neither this nor the classical viewpoint is correct, but rather that there are stable non-stoichiometric crystals in which the element of randomness arises from the disordering of units that are much larger than point defects (cf. Ariya & Popov 1962; Gadó 1963; Roth 1960; Willis 1963). The suggestion is that several stages may obtain between complete order and complete disorder (Anderson 1963, 1964; Pashley 1964) and that the latter situation exists (in metal oxides, at least) only at extremely high temperatures. The issues involved have been thoroughly discussed by Anderson (1963, 1964): the need is for more, relevant experimental data.

Historically, description of the rare earth oxide systems $RO_x + O_2$ ($1{\cdot}5 \leqslant x \leqslant 2{\cdot}0$; $R =$ Ce, Pr, Tb) has followed the same trend. Thus, intermediate phases have been observed in what were once thought to be ranges of solid solution. Attempts to rationalize their stoichiometries have been made (Bevan 1955; Baenziger, Eick, Schuldt & Eyring 1961; Honig, Clifford & Faeth 1963) but these have been handicapped by an insufficiency of accurate data: precise stoichiometries and compositional widths, if any, were not always known. However, widely non-stoichiometric phases also appeared to be stable under appropriate conditions (Bevan & Kordis 1964; Brauer & Gingerich 1957, 1960; Brauer, Gingerich & Holtschmidt 1960; Ferguson, Guth & Eyring 1954; Guth & Eyring 1954; Honig *et al.* 1963).

Previous data for the system $PrO_x + O_2$ have been analysed in an earlier paper (Hyde, Bevan & Eyring 1964). Many of them derived from comprehensive and accurate isothermal tensimetric measurements (Ferguson *et al.* 1954; Honig *et al.* 1963) which, none the less, did

not permit a complete and unambiguous resolution of the phase relations; interpretation is complicated by major hysteresis effects (Faeth & Clifford 1963; Honig *et al.* 1963). A further study of $PrO_x + O_2$ seemed to be worth while.

The extreme facility with which oxygen can be transferred between solid PrO_x and the gas phase, even at temperatures as low as 400 °C, makes the preparation of well ordered equilibrium crystals for diffraction studies difficult. By the same token isobaric experiments become attractive, particularly as oxygen pressures are in a convenient range for measurement (0 to 1 atm). The work reported here involves such a study. In addition to producing an unambiguous phase diagram for the system, the results are relevant to the broader problem of 'order-disorder' mentioned above.

2. Experimental method

An automatic recording vacuum semimicrobalance (Ainsworth, type RV) was used. The sample (approx. 2·5 g of $PrO_{1.83}$ in a platinum bucket) was suspended by about 1 m of fine Pt+10 % Rh wire from one pan of the balance into a 2 in. diameter quartz tube. A vertical tube furnace about 20 in. long was positioned around the quartz tube so that the sample was in the centre of its constant-temperature zone. The furnace tube was only slightly larger than the quartz tube, and the annulus was sealed at the top with alumina wool. This, and a plug in the bottom of the tube furnace, prevented convection and minimized thermal gradients.

The furnace temperature was controlled by a programmer actuated by a chromel-alumel thermocouple inserted into the centre of the furnace so that its junction was in contact with the furnace wall. Sample temperature was assumed to be indicated by a Pt/Pt+10 % Rh thermocouple junction inside the quartz tube and situated within 2 or 3 mm of the sample bucket.

Sample weight and temperature were recorded simultaneously and continuously on the same chart, temperature sensitivity being about ± 2 deg, weight precision $\pm 20\,\mu$g (equivalent to $\Delta x \simeq \pm 0{\cdot}0001$). At high temperature and high pressure, absolute accuracy in the weight record is commonly limited by convection effects. This source of error was investigated by doing blank runs with neodymia. Even at the highest pressures and temperatures the maximum spurious weight change (due to convection and buoyancy) corresponded with a compositional error $\Delta x < 0{\cdot}001$. It was not reproducible and therefore ignored, so that compositional accuracy is limited to $\pm 0{\cdot}001$. The higher precision over narrower temperature and pressure ranges would be expected to give more accurate compositional widths for the monophasic regions, within the limits imposed by our interpretative technique.

The praseodymium oxide (99·9 %, from Michigan Chemical Corporation, St Louis, Michigan) was purified before use by homogeneous precipitation with dimethyl oxalate from a solution of Pr^{III} in dilute nitric acid. After filtering and washing, the oxalate was ignited in a muffle furnace at *ca.* 950 °C to give $PrO_{1.833}$ when cooled in air (Ferguson *et al.* 1954; Pagel & Brinton 1929). The weighed sample was loaded on the balance, heated to 850 °C in vacuum to remove adsorbed water and carbon dioxide, and then heated at 700 °C in 1 atm pressure of hydrogen to ensure complete reduction to the sesquioxide. Since the weight was monitored during these processes, this gave one calibration point (taken as

PrO_x with $x = 1{\cdot}5000$) on the weight scale of the chart. Further heating and cooling in air re-formed the oxide Pr_6O_{11} ($x = 1{\cdot}833$): the weight of this was used only to check the composition scale, the scale being determined by the weight of $PrO_{1{\cdot}5000}$ and the balance-chart reading at that composition.

The sequence of events during a run was as follows. With the furnace at room temperature, dry cylinder oxygen was admitted to the evacuated balance system to give the desired pressure. The system was then isolated and the furnace temperature increased at a controlled rate of about $1\frac{1}{2}$ degC/min to a maximum of approximately 1150 °C. The sample was allowed to 'soak' at that temperature for $1\frac{1}{2}$ h after which time the temperature was reduced, again at a controlled rate of about $1\frac{1}{2}$ degC/min. Oxygen pressures were measured on a simple mercury manometer to ± 1 mm and are reported uncorrected. (The manometer was isolated from the balance chamber by a stopcock. This was opened only two or three times during the run to allow the oxygen pressure to be checked. Contamination of the balance and sample by mercury vapour was thus avoided.)

For this survey no attempt was made to manostat the system. However, almost all the volume of the system was at a very steady room temperature; the heating of the quartz tube by the furnace thus caused little variation in the oxygen pressure during a run, manometer readings showing an increase of 3 to 4 % at the highest temperature. A further increase, significant at low pressures, was due to loss of oxygen from the solid to the gas phase as the temperature was raised: this was measured as 3 to 4 torr. Where appropriate, corrections were applied to obtain the actual pressure at any point during a run. Such small pressure variations during the run had no qualitative effect and usually little quantitative effect on the t-x relation although, strictly speaking, the data are only approximately isobaric. While basically a classical technique, the wealth of information revealed is of a completely new order. Now that the power of the method is manifest, close manostatting would clearly be worth while.

Each run lasted 24 to 30 h. (It was not necessary always to cool to room temperature between runs, since rapid oxygen exchange usually requires temperatures in excess of *ca.* 350 °C.) In all, twenty-five runs were made; these covered the pressure range 'zero' to 1 atm. 'Zero' pressure refers to the situation obtaining when a cold sample (usually $x = 1{\cdot}80$ to $1{\cdot}81$) in an evacuated, isolated system was heated and cooled through the normal programme. In such a case, the only gaseous oxygen present was that released from the solid as it was heated (see above). This was almost completely re-absorbed on cooling.

Weight and temperature readings, W and t, were taken off the chart records at 5 min intervals for the whole of each run (every 1 to 2 min during rapid weight changes). These tabulated data, 300 to 350 points per run, were then plotted as 'isobars' of W against t. The collection of isobars was used to obtain a first estimate of homogeneity and temperature stability ranges of the separate phases, and to resolve the detailed behaviour of the system. Accurate composition and temperature values were then taken from the original charts and used to construct the t-x projection of the phase diagram, the full p-x-t diagram, etc. The nature of the deductive processes will be described.

3. Results

(a) *Introductory remarks*

Initially it must be assumed from the nature of the experiments that non-equilibrium data were obtained. However, there are many sections of the isobars in which oxidation and reduction paths are coincident or very nearly so (see figure 1). For such regions we assume that the deviations from equilibrium are too small to be significant. A wealth of observation confirms that this is to be expected *when the solid is monophasic*: also, and in contrast, that departure from equilibrium may be quite marked when the solid is diphasic† (Ferguson *et al.* 1954; Hyde *et al.* 1964; and especially Honig *et al.* 1963; Czanderna 1957; and Faeth & Clifford 1963). Against this background, and in terms of the usual phase rule criteria, our approach is the following.

Near-horizontal lines, i.e. marked change of composition at nearly constant temperature, are interpreted as indicating diphasic regions of the phase diagram—classically 'univariant'. Near-vertical lines, composition nearly independent of temperature, are assumed to prove the existence of discrete 'compounds' of narrow homogeneity range, and therefore highly ordered structurally. In the former case heating and cooling paths are markedly separated; in the latter they are usually coincident. These two types of behaviour correspond respectively to hysteresis and reversibility in the *equilibrium* pressure/composition isotherms of Faeth & Ferguson. The situation is less clear-cut with a line of intermediate slope. Where the heating and cooling paths are coincident we assume the presence of a monophasic solid of wide composition range (solid solution, disordered non-stoichiometric phase). In the absence of reversibility a more careful analysis of the behaviour is called for.

Overall, our results confirm the existence of intermediate stoichiometric phases, PrO_x, at compositions $x \simeq 1{\cdot}71$, $1{\cdot}78$, $1{\cdot}80$, and $1{\cdot}83$, and of two wide-range non-stoichiometric phases: phase compositions and designations are listed in table 1. In addition they show, for the first time, the presence of an intermediate phase with $x = 1{\cdot}81_8$. Honig *et al.* (1963) reported a phase with $x = 1{\cdot}82$, but it is now clear that this was simply one composition in the range of the widely non-stoichiometric α phase.

(b) *Brief survey*

Runs are designated by a number which is the nominal oxygen pressure at the commencement of the run, measured in millimetres of mercury. Four representative runs, 650, 205, 45 and 10, have been selected to show the various features of the phase diagram. The data are reproduced in figure 1. Figure 2 is the derived *t*-*x* projection of the phase diagram.

(i) *Run* 10

The starting composition for this run was $PrO_{1{\cdot}80}(\epsilon)$, the end product of a previous run at a lower pressure. Initial heating produced some oxidation, sluggish because the temperature was low. Before conversion to a more oxidized phase was complete its dissociation temperature was exceeded and the sample reverted to ϵ. At 497 °C this decomposed to give ζ ($PrO_{1{\cdot}78}$) which, in turn, decomposed to ι ($PrO_{1{\cdot}71}$) at 588 °C. Each of these three phases is

† The complete phase system is termed two-phase, three-phase, etc.; condensed phase equilibria are described as monophasic, diphasic.

TABLE 1. PHASE NOMENCLATURE IN THE PrO_x+O_2 SYSTEM

phase composition, x in PrO_x	designation
disordered, non-stoichiometric phase, $2{\cdot}00 \gtrsim x \gtrsim 1{\cdot}72$	α, α^m
1·833 (ordered)	β
1·83 (disordered)	$\beta'(\equiv\alpha)$
1·818	δ
1·800	ϵ
1·778	ζ
1·714	ι
wide-range, disordered, non-stoichiometric phase $1{\cdot}7 \gtrsim x \gtrsim 1{\cdot}6$	σ, σ^m
1·500 (A type)	θ
1·500 (C type)	ϕ

The superscript 'm' indicates metastable existence of a phase: according to our analysis of the behaviour of this system, σ^m and α^m are particularly liable to occur.

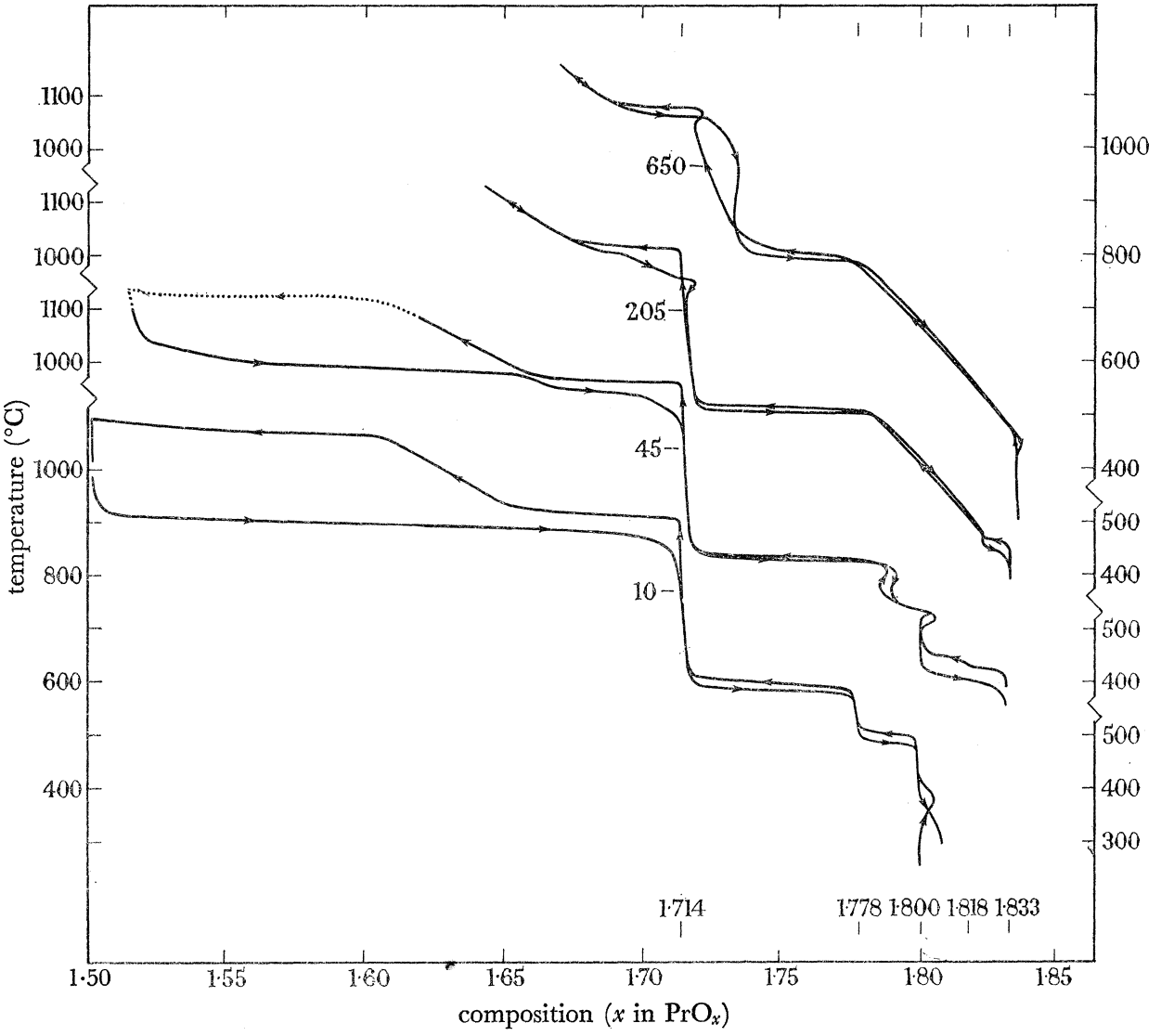

FIGURE 1. Representative isobaric runs; nominal oxygen pressure 10, 45, 205 and 650 torr.

seen to span a very narrow composition range. At 906 °C ι reduced to σ whose composition varied between about $PrO_{1\cdot65}$ at 930 °C and $PrO_{1\cdot60}$ at 1068 °C, at which temperature it decomposed to the sesquioxide.

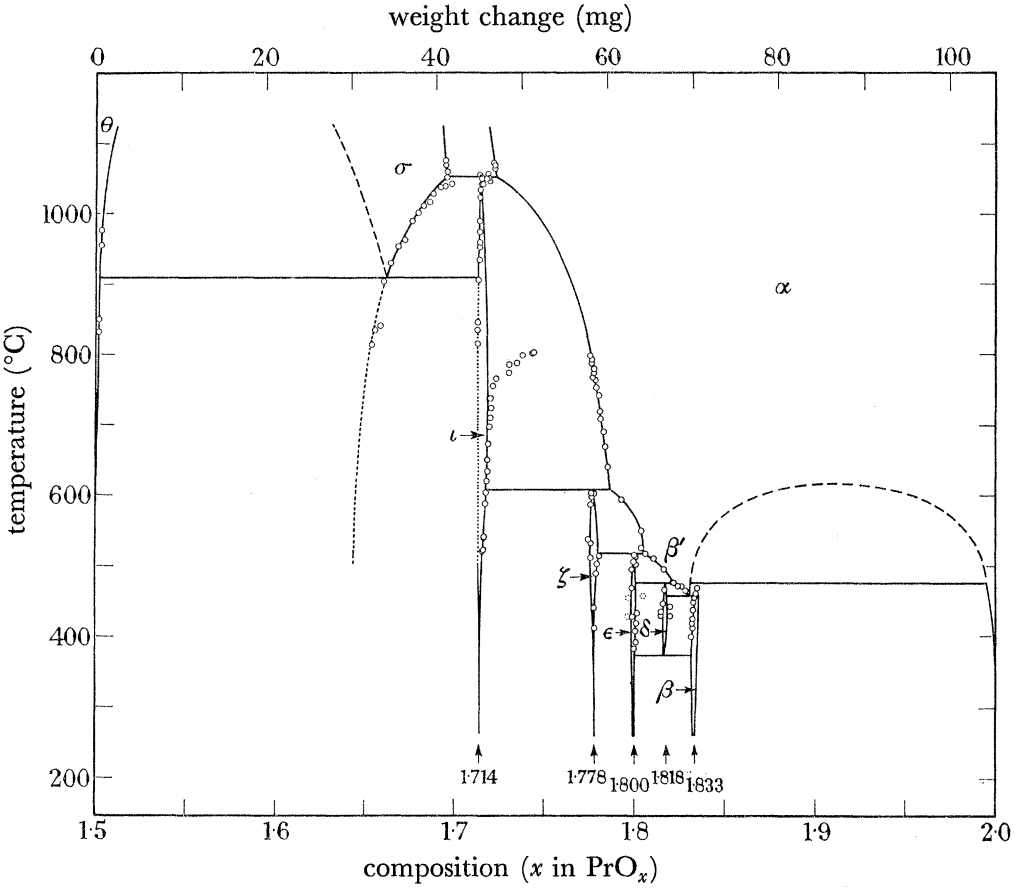

FIGURE 2. Projection of the praseodymium oxide+oxygen phase diagram on to the temperature-composition plane. ○, Experimental points from the isobars; ——, phase boundaries, stable; – – –, phase boundaries, stable, assumed; - - - -, phase boundaries, metastable.

Cooling produced no change in composition until a temperature of 945 °C was reached, then slow oxidation began. The oxidation rate increased dramatically with a further slight reduction in temperature, becoming slower again as the composition of the ι phase (the end product of this reaction) was approached. The sharp onset of oxidation after a period of uneventful cooling is the isobaric analogue of the 'break pressure' effect observed by Honig *et al.* (1963) in their isothermal studies. This, and the absence of σ during cooling, will be discussed later. Below 750 °C the heating and cooling curves in the ι phase region were almost coincident, and even closer coincidence was evident for the ζ and ϵ phases. However, hysteresis was observed for the diphasic regions $\iota+\zeta$ and $\zeta+\epsilon$. At 385 °C ϵ began to oxidize across a diphasic region, but the low temperature quenched the reaction before it was complete.

(ii) *Run* 45

Beginning with the β phase ($PrO_{1\cdot83}$), this decomposed at 420 °C to δ ($PrO_{1\cdot82}$) which in turn decomposed almost immediately to ϵ. The subsequent decompositions of ϵ and ζ

occurred *in oxidation* across descending three phase blades (respectively $\epsilon+\alpha$ and $\zeta+\alpha$), so that the production of ζ and ι took place *in reduction* across rising $\zeta+\alpha$ and $\iota+\alpha$ blades respectively.† The ι phase decomposed at 960 °C to σ, whose composition changed from $PrO_{1\cdot67}$ at 975 °C to about $PrO_{1\cdot60}$ at 1070 °C, at which point it in turn decomposed. The product of this last decomposition was the sesquioxide, although reduction to $PrO_{1\cdot5}$ was not complete even at the end of the 'soak' period.

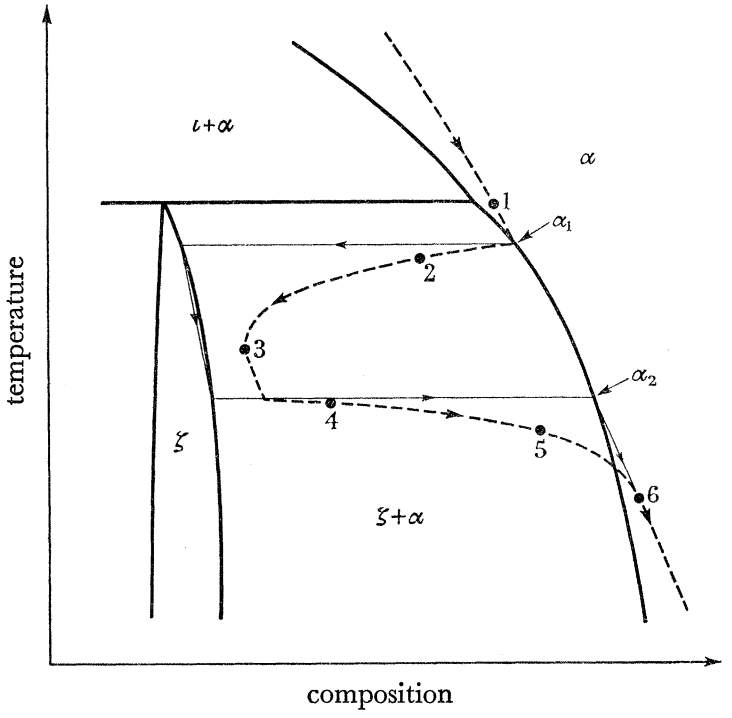

FIGURE 3. Schematic temperature-composition projection of reaction path for the process $\alpha \rightarrow \zeta \rightarrow \alpha$: ——, phase boundary; ⟶⟶, equilibrium path; – – ⟶ – –, experimental path.

This being so, the sample was a mixture of $PrO_{1\cdot5}$ and σ as cooling started. The σ remnant oxidized with decreasing temperature, but the sesquioxide was unaffected until the 'break temperature' of about 1050 °C was reached; then it oxidized rapidly to σ. The isobar (figure 1) shows both of these processes: the partial arrest at the low temperature end of the σ phase region indicates completion of the $PrO_{1\cdot5} \rightarrow \sigma$ oxidation. As the temperature fell past 950 °C σ oxidized to ι. Oxidation and reduction paths along the ι surface are indistinguishable between 860 and 730 °C and almost so down to 645 °C. At 634 °C ι oxidized to α.

The run then shows exceptions to the general rule that *W-t* plots are reversible in single-phase regions, for ζ and to a lesser degree for ϵ. In these cases we are concerned with simultaneous processes involving coexisting phases; e.g. for the successive processes $\alpha \rightarrow \zeta \rightarrow \alpha$, ζ starts to decompose before its formation is complete (see figure 3). This will concern us later. The lack of reversibility in the δ-phase region has a somewhat different cause; ϵ apparently oxidized directly to β during cooling.

† Three-phase equilibria produce a surface (p, x, t) generated by a straight line moving parallel to the x axis and called a *blade* or *strip*. A 'descending' or 'falling' blade has $dp/dt < 0$; a 'rising' blade has $dp/dt > 0$.

(iii) *Run* 205

The initial composition of the sample was again $PrO_{1\cdot83}$. With increasing temperature this β phase decomposed at about 460 °C to produce δ, although the appropriate equilibrium composition was not attained before δ decomposed to α, in oxidation across the descending $\delta+\alpha$ blade. Pure α persisted from 480 to 705 °C, its composition varying almost linearly with temperature from about $PrO_{1\cdot826}$ to $PrO_{1\cdot782}$. There was no indication of the presence of the ϵ and ζ phases which appeared prominently at lower pressures. At 710 °C α decomposed to ι, the latter persisting to 1020 °C with very little change in composition. Then ι reduced to give a σ phase of composition $x \simeq 1\cdot675$: σ obtained, with a steady composition decrease, to $x \simeq 1\cdot645$ at 1130 °C—the highest temperature attained in this run. With decreasing temperature the oxidation path of the σ phase was parallel and close to, but not quite coincident with, the reduction path. The reason for the lack of perfect reversibility is uncertain; some runs do show reversible behaviour for the σ phase.†

At a composition $x = 1\cdot68$ and a temperature of 1011 °C there was a 'break' in the cooling curve as σ started to oxidize. At 1000 °C ($x \simeq 1\cdot692$) a linear path of intermediate slope was resumed, continuing to 960 °C and a composition of $x \simeq 1\cdot71$ (cf. run 45). At this point the oxidation curve broke across the reduction curve in the temperature interval 960 to 950 °C, the composition increasing to $x \simeq 1\cdot72$—i.e. to the right of the ι phase composition. As the temperature continued to fall the sample reduced, and the cooling and heating curves almost coincide down to 785 °C, just preceding the oxidation of ι to α. Slight hysteresis was observed in this latter diphasic region. At 473 °C the partial conversion of α to δ occurred in reduction; and at 461 °C δ decomposed to β.

The heating and cooling curves are very different in the region 900 to 1050 °C,

$$1\cdot68 < x < 1\cdot72,$$

and this merits some comment. Anticipating a subsequent argument, we interpret the breaks in the cooling curve at 1011 and 960 °C as indicating the oxidations $\sigma \rightarrow \iota$ and $\sigma^m \rightarrow \alpha^m$ respectively. The reversal at 950 °C is then a consequence of α^m reverting to ι. The linear path between the two breaks (starting at *ca.* 1000 °C and $x \simeq 1\cdot692$) might suggest a monophasic region lying between the composition limits of σ and ι. However, the breaks imply the presence of both σ^m and ι. An explanation for this anomaly is given below (§ 4 (*b*)).

(iv) *Run* 650

The run started with β of composition $x = 1\cdot836$, the end product of a previous run at higher pressure. On heating, slight oxidation occurred (not detectable in figure 1) followed by reduction at 342 °C .This reflects the start of slow oxidation of β to PrO_2 which then reverted to β. (It should perhaps be emphasized that figure 1 is on a very much smaller scale than the chart records. The composition range in the figure covers about $7\frac{1}{2}$ widths of recorder chart—an accumulated pen deflexion of 6 ft. 3 in.) At 470 °C β transformed to α with a very small change in composition, also undetectable in figure 1, and the subsequent

† It has since been discovered that the cause of the discrepancy is slight 'pickup' by the thermocouple from the furnace-winding current; this is greater in heating (higher current) than in cooling (lower current at same temperature).

PHILOSOPHICAL TRANSACTIONS OF THE ROYAL SOCIETY A MATHEMATICAL, PHYSICAL & ENGINEERING SCIENCES

isobaric path lay on the α surface up to 795 °C, at which temperature α reduced to ι. This conversion was slow and still incomplete when, at 1051 °C ($x \simeq 1{\cdot}72$), the ι phase reoxidized across the descending $\iota+\alpha$ blade. At 1065 °C α decomposed to σ of composition $x \simeq 1{\cdot}695$. The σ phase persisted to the maximum temperature and, on cooling, perfect reversibility was achieved until it oxidized at 1069 °C. Again anticipating what follows, we believe the product of this oxidation was α which, as the temperature was lowered further, became metastable with respect to ι. The isobar shows (in cooling) the gradual conversion of α to ι, but before this was complete the temperature fell to the point where α again became stable with respect to ι, so that reversion to α occurred across the rising $\iota+\alpha$ blade ($t = 800$ °C). Thus, in the region where α is unstable with respect to ι, the isobar lies well to the right of the ι composition range. In contrast, close reproducibility between heating and cooling of the stable α phase is again notable.

There is much evidence of the system showing a 'reluctance' to leave the free energy surface describing the α phase. We attribute this to disorder in α, in contrast with the high degree of order obtaining in the other phases ($\beta, \delta, \epsilon, \zeta, \iota$) in the same composition range. A further example on this same cooling curve is the deviation from the heating curve that began at approx. 470 °C. It obviously results from the system persisting on the (metastable) α^m-phase surface, a reversal at 445 °C being due to the ordering of α^m to give β. From 420 to 360 °C the heating and cooling curves were identical.

4. Collation and interpretation

(*a*) *Orthodox behaviour*

The broad significance of certain features of the isobars is clear: these include indications of the intermediate phases β, δ, ϵ, ζ and ι and of the diphasic regions which separate them; of the non-stoichiometric phases α and σ; and of the diphasic regions separating α and ι and, particularly in reduction, ι and σ. Other features are less easily interpreted, especially the various patterns of behaviour observed at different pressures in the composition range $1{\cdot}67 < x < 1{\cdot}73$ and reproduced in figure 4. The system is clearly far from equilibrium, either in oxidation or in reduction; possibly in both. Non-equilibrium behaviour also appears at higher x values: thus we have commented on the persistence of α at higher temperatures.

It has been suggested that many of the data describe states of the system close to equilibrium, especially those for monophasic regions. Moreover, those experimental temperatures (T_e °K) at which a monophasic solid first becomes obviously unstable with respect to its decomposition product differ by no more than 15 degC as between oxidation and reduction across a given diphasic region. Usually agreement is within 5 to 10 degC, and in many cases within the error of reading the chart. (This point is assumed to be given by the intersection of the extrapolated curves for the mono- and diphasic regions, cf. the heating curve in figure 6.) This suggests that the *onset* of a phase reaction occurs under conditions close to equilibrium for that process, and we have therefore investigated the function $RT_e \ln p$ for well defined diphasic regions. Our own results have been augmented by those of Pagel & Brinton (1929) for the $\beta+\alpha$ equilibrium at high oxygen pressures, and by the data of Faeth (1961; see Honig *et al.* 1963) for the oxidation of *A*-form sesquioxide, θ.

The graphs of $RT_e \ln p$ against t_e demarcate monophasic regions that are not quite coincident in heating and cooling. Separate plots are therefore given in figures 5 (*a*) and (*b*). This may be a consequence of hysteresis in phase transformations of the $PrO_x + O_2$ system, already well established by Faeth's work. An averaged partial molar free energy diagram (figure 5 (*c*)) is utilized in the following discussion, i.e. hysteresis effects are largely ignored.†

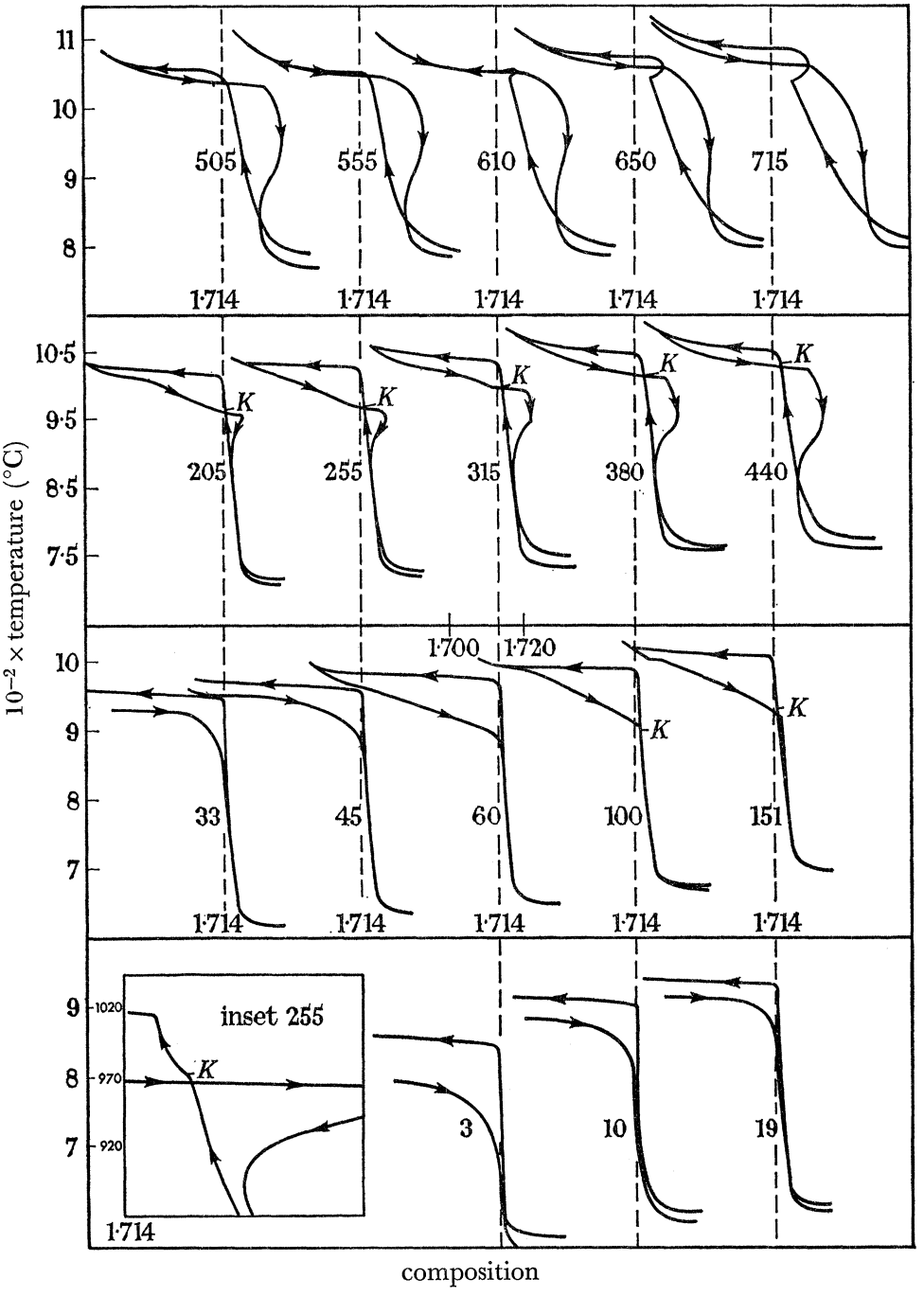

FIGURE 4. Portion of isobars in the composition range *ca.* $PrO_{1·68}$ to $PrO_{1·74}$ on an expanded composition scale. (The run number against each curve is the nominal oxygen pressure in torr.)

† The difference between figures 5 (*a*) and (*b*) is not simply a shift of origin; the shapes of the monophasic regions are changed.

It is significant that *all* the $RT_e \ln p$ values are 'well behaved', including those extracted from the more complex, non-reversible sections of the isobars. Accordingly, *every* break is recorded in figure 5. (In contrast, the phase composition limits are correct only for the

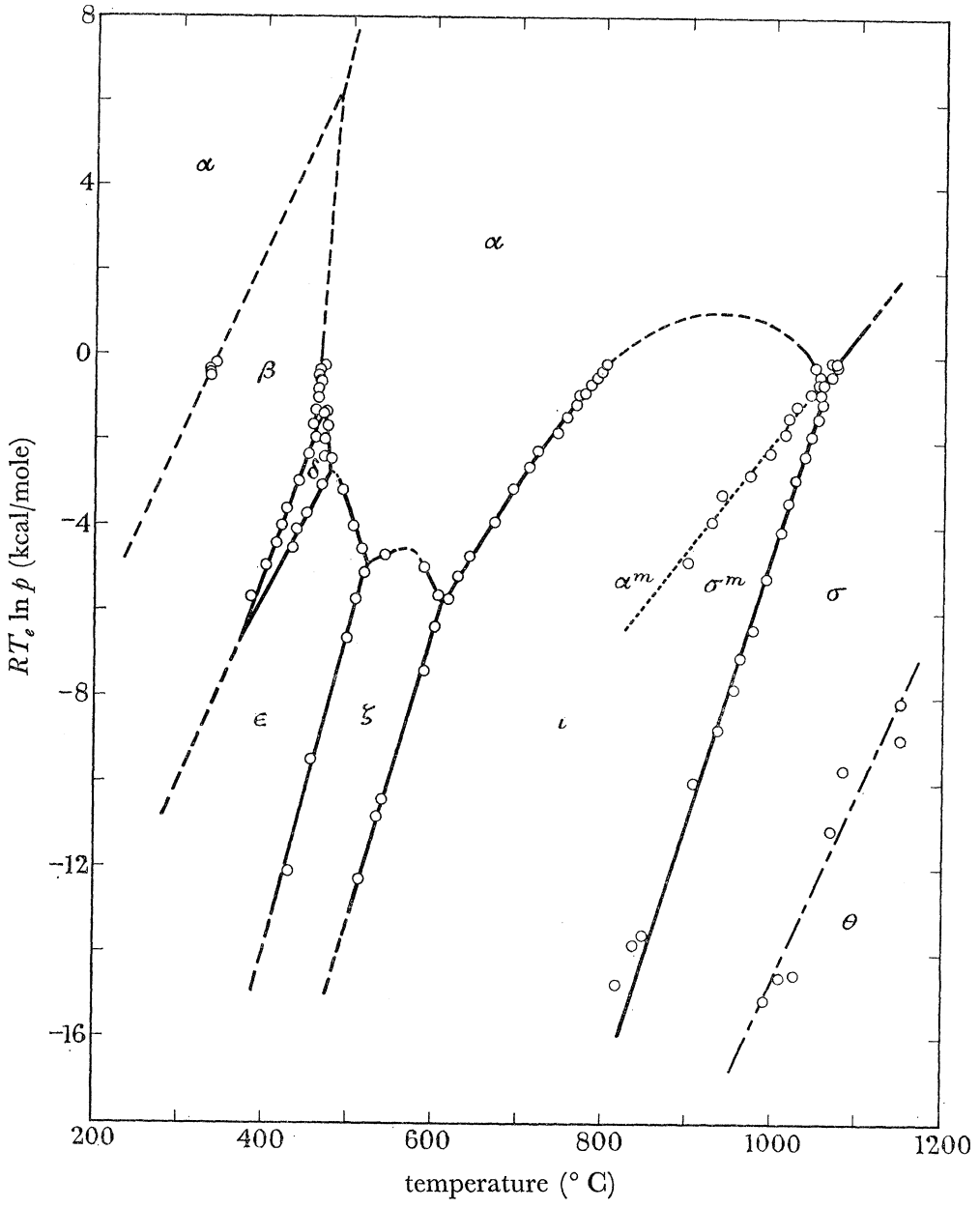

FIGURE 5*a*. Partial molar free energy of oxygen for the various phase reactions, as a function of temperature and oxygen pressure. Heating. ○, Experimental points; ——, phase boundaries, stable; — — —, phase boundaries, stable, assumed; – – – –, phase boundaries, metastable; — – — – $\sigma \rightarrow \theta$ conversion.

reversible sections; so that most of the other x values are omitted from figure 2.) This consistency substantiates the suggestion that a phase reaction always initiates under equilibrium conditions.

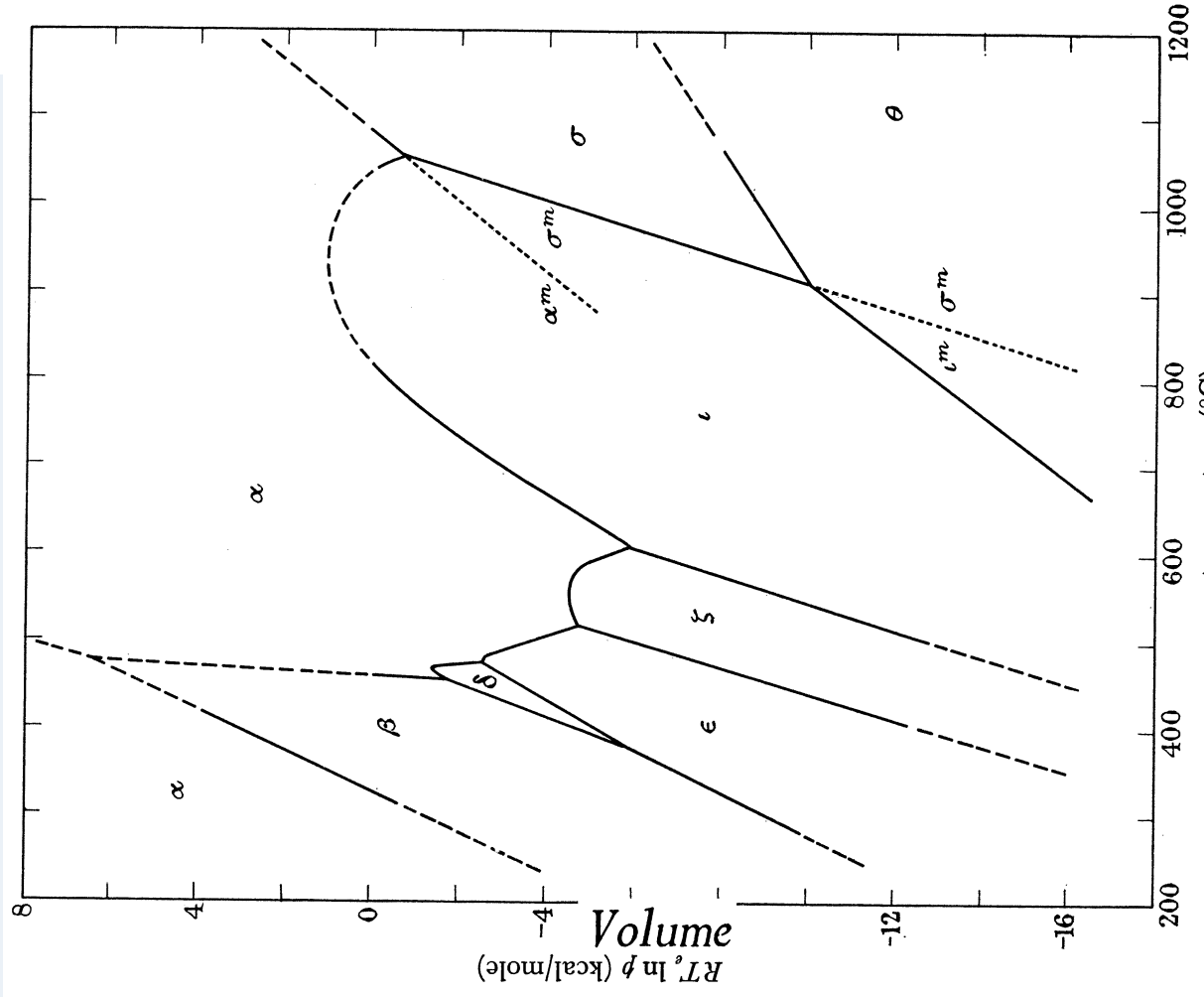

FIGURE 5b. Partial molar free energy of oxygen for the various phase reactions, as a function of temperature and oxygen pressure. Cooling. ○, experimental points, this work; ●, experimental points, Faeth (1961); ——, phase boundaries, stable; — — —, phase boundaries, stable, assumed; – – – – –, phase boundaries, metastable.

FIGURE 5c. Partial molar free energy of oxygen for the various phase reactions, as a function of temperature and oxygen pressure. An 'average' of figures 5 (a) and (b).

(*b*) *Irregular features*

Examination of the isobars surveyed in § 3 (*b*) suggests, and a careful scrutiny of every isobar confirms, the presence of a *leitmotif* in all cases of anomalous behaviour. Each complex, irreversible isobaric segment concerns a phase reaction involving a disordered phase (α or σ) and an ordered phase (β, δ, ϵ, ζ or ι): the complexities stem from an order-disorder transformation. Furthermore, *the direction is always disorder → order*; the reverse reactions occur in an orthodox manner. This observation suggests a simple crystallo-chemical explanation of the anomalies, which also emphasizes the extreme importance of structural relationships between the reactant and product phases in solid-state reactions.

For the PrO_x phases, the finer structural details are still unknown; however sufficient general understanding is available for our present purpose. All the phases listed in table 1 (except θ; hexagonal *A*-form Pr_2O_3) have cation lattices almost identical with that in the fluorite-type PrO_2. Oxygen deficiency is accommodated by a reduction in the average coordination number of the cations, i.e. by 'anion vacancies'. The *C*-type sesquioxide, ϕ, has a structure which may be regarded (Pauling & Shapell 1930; Fert 1962) as fluorite-type with a proportion (25 %) of the anion sites vacant and ordered. It seems certain that β, δ, ϵ, ζ and ι may be similarly regarded. PrO_2 and α are face-centred cubic, ϕ and σ are body-centred cubic; the remaining phases are of lower symmetry (see below). The consequences are best appreciated by considering the most involved case of anomalous behaviour —the cooling curves in the region $1{\cdot}67 < x < 1{\cdot}73$, figure 4. (We believe that the heating curves in the same region are well behaved.) These segments concern the oxidation $\sigma \rightarrow \iota$: the reactant has cubic symmetry, the product is rhombohedral. In the product the pseudo-fluorite cell is elongated along *one* of its *four* body diagonal directions. Multiple coherent nucleation of ι in a single crystal of σ will therefore result in ι nuclei with their trigonal axes randomly distributed over all four $\langle 111 \rangle$ directions of the σ matrix. This randomness will be reinforced by the consequent minimizing of strain energy, as Pashley (1964) has pointed out in describing an analogous situation. While the nuclei are still small the course of the reaction will not be affected (cf. runs 45 and 205 in figure 1). As they grow their boundaries will eventually meet, at which stage further growth will be inhibited. Adjacent microdomains of ι will be twinned, and they may well isolate, by complete enclosure, microdomains of σ. The enclosed σ microdomains will be subject to isotropic stress so that their conversion to ι of any *one* orientation is prevented. The 'single crystal' is, in a sense, diphasic. Such a situation is metastable, but passage to complete equilibrium (a single crystal of ι with unique orientation) may be impossible. Reorientation of three-quarters of the existing ι microdomains would require cooperative fluctuations of quite impossibly large magnitude.

The interlocked microdomains of ι and σ will both be in equilibrium with the gas phase so that their compositions, particularly that of σ, will change with changing temperature as the run proceeds. Apparently the balance between microdomain sizes is also temperature dependent since, in most isobars, the segment concerned shows a composition more sensitive to temperature than that of σ (or ι). Although two 'phases' are present the crystal exhibits bivariant behaviour.

This model accounts for the apparently monophasic segments in the cooling curves at about $x = 1{\cdot}70$. As the temperature falls the ι microdomains expand at the expense of σ (cf.

above) so that eventually pure ι obtains (runs 45 to 100, figure 4). At higher oxygen pressures however another process intervenes (runs 151 to 315, figure 4): before σ is entirely eliminated by the expansion of ι microdomain boundaries, it oxidizes to α (i.e. $\sigma^m \rightarrow \alpha^m$) so that the overall composition surpasses that of ι. Conclusive evidence for this assertion is provided by the fact that $RT_e \ln p$ values for this last break lie on an extrapolation of the line for $\sigma+\alpha$ *at equilibrium* (cf. figure 5(*b*)). Considering the strain that must result from coherence, this observation is somewhat surprising.

Behaviour of the type shown in figure 3 is analogous; in this case the ordered *product* microdomains decompose before the metastable reactant has completely converted.

The stability, albeit metastability, of the microdomain texture must be emphasized. The shape of the isobars is not sensibly affected by change in heating or cooling rates. A careful examination of similar behaviour in the system TbO_x+O_2 (carried out after the present work; Hyde & Eyring 1965) showed that the point at which the $\sigma \rightarrow \iota$ reaction was completed also had well-behaved $RT_e \ln p$ values. (In that case $\sigma^m \rightarrow \alpha^m$ does not intervene.) These values were independent of the isobaric path; whether around the hysteresis loop, or along a scanning curve inside the loop. Unlike the microdomain model proposed by Ariya & Popov (1962) for TiO_x, the present situation cannot be completely mobile, otherwise passage to true equilibrium would occur. The term *pseudo-phase* has been adopted for such a diphasic, bivariant solid (Hyde & Eyring 1965). Pseudo-phases are, we believe, not uncommon: they provide a simple explanation for reactions observed to be bivariant in one direction, but monovariant when reversed (cf. PbO_x+O_2; Anderson & Sterns 1959). The high pseudo-symmetry observed for the pseudo-phase (PbO_x, Katz 1950; PrO_x, Guth, Holden, Baenziger & Eyring 1954) indicates the fineness of the microdomain texture.

The appearance of a pseudo-phase during a phase reaction demands two prerequisites:

(1) Coherence between the reactant and product, which in turn requires a close structural relationship between them. (In Mackay's (1961) terminology the reaction described above is a *topotactic* transformation.)

(2) The possibility of sufficient orientational and/or translational degeneracy in locating the product lattice on that of the reactant. (A minimum degeneracy of four is necessary for the microdomain texture to be stable; cf. Bragg (1940), quoted by Guttman (1956).)

Coherence in the oxidation and reduction of PrO_x phases is demonstrated by Schuldt's (1957) observation that there is no concomitant change in surface area. It has already been suggested (see, for example, Everett & Nordon 1960) that lattice strain resulting from coherence will cause hysteresis in phase transformations. Conversely, lack of coherence, as shown by a reduction of crystal size—increase in surface area—would be expected to prevent hysteresis.

Using these ideas we now interpret the isobaric behaviour of PrO_x+O_2 in detail.

(*c*) *Synopsis*

(i) *The region* PrO_2 *to* $PrO_{1.75}$

At all but the lowest pressures the starting composition for the heating runs is $PrO_{1.830}$ to $PrO_{1.836}$—the ordered β phase at temperatures below *ca.* 455 °C. As the temperature is increased in this region, the composition remains virtually constant until the first sharp reduction break occurs. At the highest oxygen pressures slow oxidation to the dioxide

begins, but reverses when a temperature of approx. 335 C° is attained. These changes are not apparent in the small-scale diagrams. At pressures ranging from *ca.* 30 to 205 torr, the δ phase ($x \simeq 1{\cdot}82$) is in evidence, and we have assumed the break temperature to be that for the $\beta \rightarrow \delta$ transition. In run 19 there is no direct evidence for the formation of δ from β in reduction, but rather a suggestion that at this low pressure ϵ is formed directly. The implication is that δ undergoes a eutectoid decomposition into $\beta+\epsilon$ at about 410 °C. However, the value of $RT_e \ln p$ at the break from β falls on the $\beta+\delta$ equilibrium line (figure 5(*a*)),

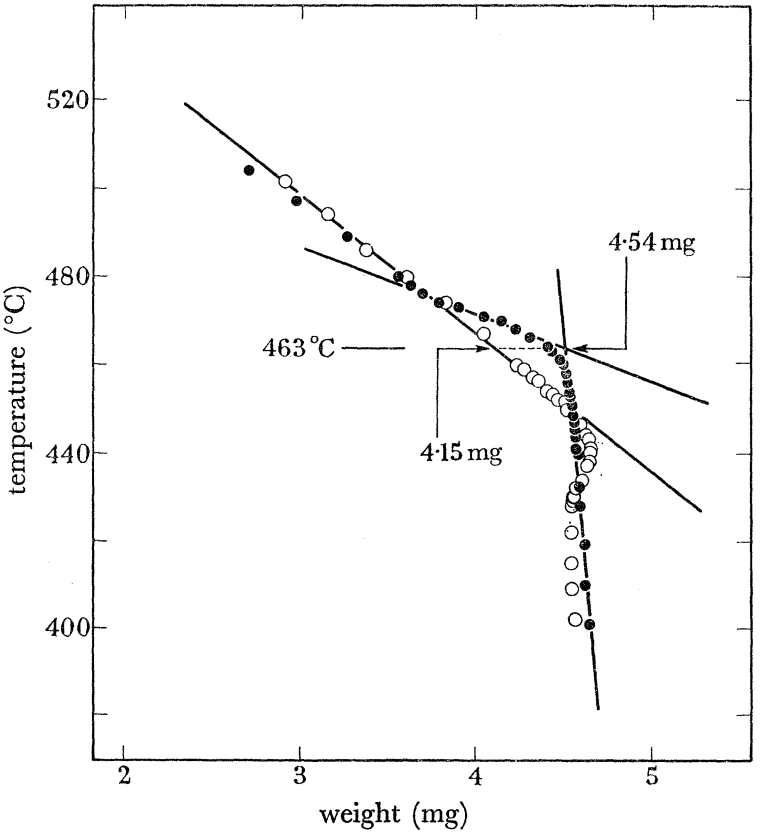

FIGURE 6. Transition $\beta \rightleftharpoons \beta'$ ($\equiv \alpha$), plotted on a much expanded composition scale. Composition range, *ca.* $PrO_{1{\cdot}825}$ to $PrO_{1{\cdot}835}$. Oxygen pressure = 505 torr. ●, heating; ○, cooling.

showing that β does reduce to δ in this case. The absence of a positive indication of δ in the isobar is probably a consequence of rather low oxygen mobility at such a low temperature (401 °C), together with its rapid decomposition to ϵ (at 412 °C): the 'lifetime' of δ (the time to traverse its narrow temperature range of stability at $1\frac{1}{2}$ degC/min) is comparable with the relaxation time of the anion lattice. Nevertheless, extrapolation of the curves of $RT_e \ln p$ against t_e lines for the $\beta+\delta$ and $\delta+\epsilon$ equilibria shows that the eutectoid reaction $\delta \rightarrow \beta+\epsilon$ *does* take place, but at a slightly lower temperature, ~ 378 °C, $p \simeq 8$ torr (see table 2).

At pressures greater than *ca.* 205 torr, a clear break from β occurs, but again the δ phase is not indicated unambiguously. The $RT_e \ln p$ values now fall on another steeply sloping line, which confirms that in these circumstances δ does not form. For these higher pressure runs large-scale *W-t* plots of this region (such as figure 6) reveal the presence of a narrow three-

phase blade ($\beta'+\beta+O_2$)† which extends to high pressures over a very small temperature range. The phase relations are shown in figures 7 and 8. Experimental values of x in figure 7 (a) were obtained from the original chart records: the left-hand boundary of the $\beta'+\beta$ blade was assumed to be given by the composition of the solid at the same temperature on cooling, as that at which the $\beta \rightarrow \beta'$ transformation commenced on heating (see figure 6). The maximum compositional width of the $\beta'+\beta$ blade is $\Delta x \simeq 0{\cdot}004$, decreasing to $\Delta x \simeq 0{\cdot}0006$ at an oxygen pressure of 600 torr. We estimate that the invariant four-phase

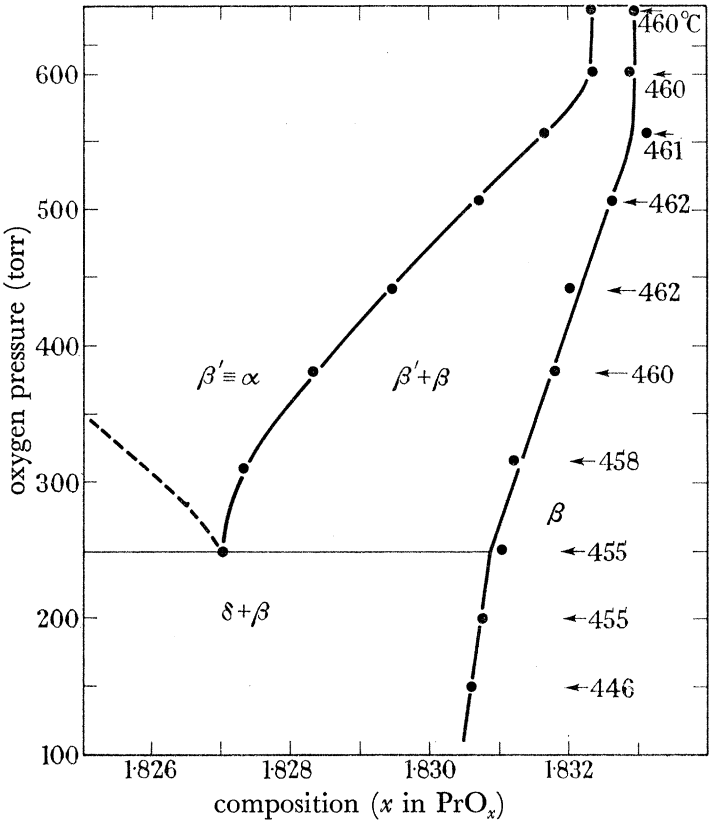

FIGURE 7a. Projection of the $\beta \rightleftharpoons \beta'$ region of the phase diagram on to the pressure-composition plane.

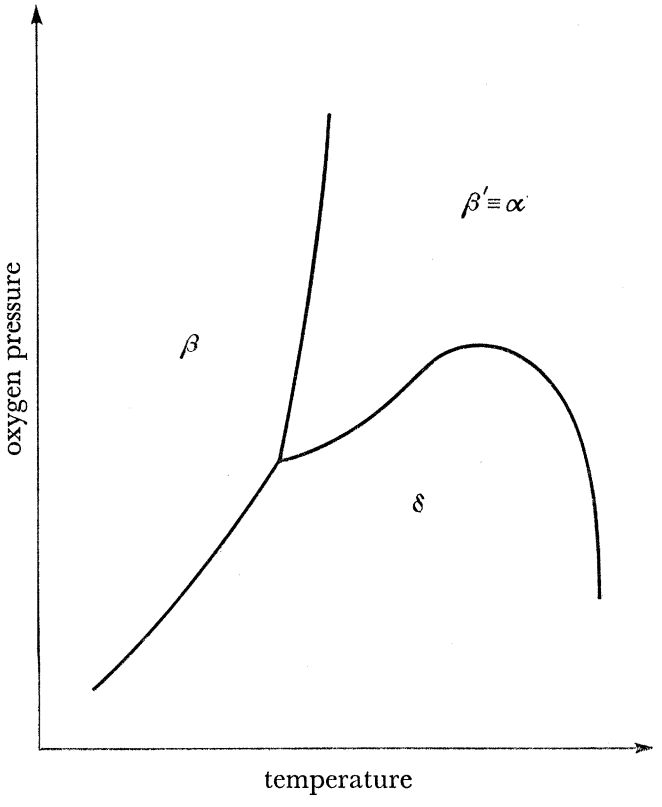

FIGURE 7b. Projection of the $\beta \rightleftharpoons \beta'$ region of the phase diagram on to the pressure-temperature plane, showing the 'descending' blade ($\beta+\delta+O_2$).

equilibrium ($\delta+\beta'+\beta+O_2$) occurs at a temperature of 456 °C and an oxygen pressure of about 228 torr. In the W-t plots the diphasic region $\beta'+\beta$ is less obvious in oxidation than in reduction; in fact, for runs 315 to 650 it does not appear on cooling; the β' phase persists (metastably) without a break, before converting to β at lower temperature. In some cases, at the highest pressures, this conversion occurs in *reduction* (cf. figure 6 and § 3 (b) (iv), run 650).

To complete this side of the phase diagram the present results may be supplemented from various sources. These include previous X-ray diffraction (Guth *et al.* 1954; Sieglaff & Eyring 1957) and high-pressure tensimetric studies (Simon & Eyring 1954) and, by analogy, the behaviour of the system CeO_x+O_2 in the composition range $1{\cdot}81 \leqslant x \leqslant 2{\cdot}00$ (Bevan

† β' is disordered β (i.e. α) on the 'left-hand side' of β. It is convenient to thus distinguish it from α on the 'right-hand side' of β (i.e. $PrO_{2-\Delta}$) in this part of the phase diagram.

PHILOSOPHICAL TRANSACTIONS OF THE ROYAL SOCIETY A MATHEMATICAL, PHYSICAL & ENGINEERING SCIENCES

1955; Brauer & Gingerich 1957; Brauer *et al.* 1960; Brauer & Gingerich 1960; Bevan & Kordis 1964). A plausible diagram for the region $PrO_{1.81}$ to PrO_2 has been constructed on this basis and is shown schematically and in isometric view in figure 8. Owing to the

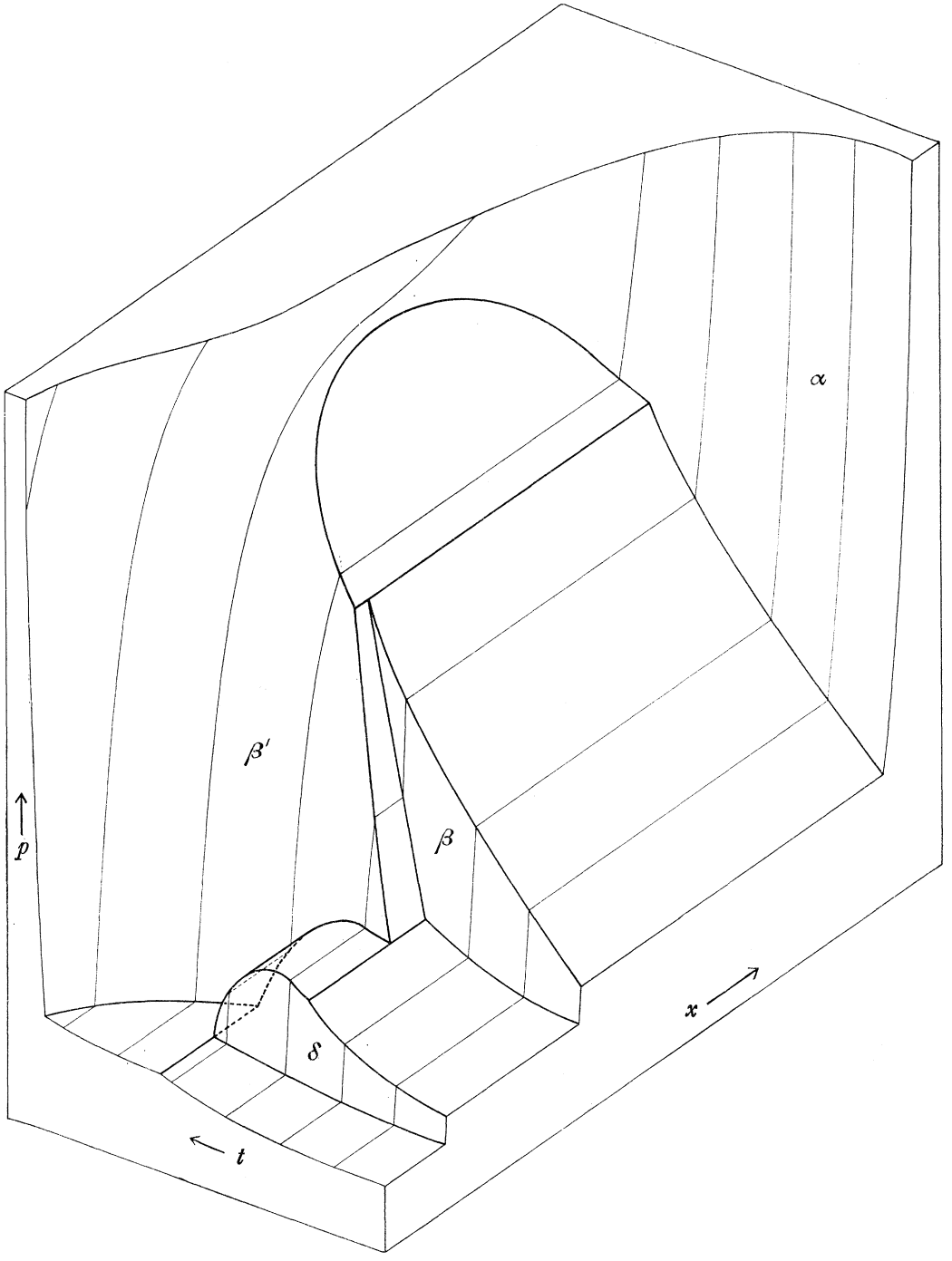

FIGURE 8. Isometric view of the surface (*p-x-t*) of the phase diagram in the composition range, *ca.* $PrO_{1.81}$ to $PrO_{2.00}$: thick line, phase boundaries; thin line, isothermal contour.

extremely high pressures obtaining, no *p-t* data are available for the miscibility gap which occurs in the α-phase region (i.e. $\beta'+\alpha$). Rough data for a few temperatures are available for the $\beta+\alpha$ region (Pagel & Brinton 1929; Hyde, Garver, Kuntz & Eyring 1965) and these

are incorporated in figure 5 (*b*). Uncertain extrapolation of this line and that for the $\beta'+\beta$ region gives the approximate conditions for the peritectoid decomposition of β into the two α phases on either side of the miscibility gap, $\beta \rightarrow \beta' + \alpha$, as $t = 476\,^{\circ}\mathrm{C}$, $p \simeq 73$ atm. Obviously the proposed consolute ($\beta' \equiv \alpha$) pressure is extremely high, even if the consolute temperature is only 585 °C as suggested by Sieglaff & Eyring (1957).

Heating at low pressures reduces δ to ϵ. In runs 150 and 200 it decomposes, *in oxidation*, to give $\alpha\,(=\beta')$. Thus the presence of a $\delta+\alpha$ falling blade is established. It terminates at an invariant quadruple axis ($\epsilon+\delta+\alpha+O_2$) at about 137 torr, 477 °C. Figure 5 shows that there is a rising $\delta+\alpha$ blade with a pressure range of approximately 230 to 310 torr.

The ϵ phase ($x=1{\cdot}80$) is present from extremely low pressures up to 100 torr. The evidence for an $\epsilon+\alpha$ falling blade is unequivocal at 45, 60 and 100 torr, but there is no definite evidence for an $\epsilon+\alpha$ *rising* blade. Figure 5 shows that a rising blade, if it does exist, must be very short. At 519 °C, $p \simeq 38$ torr, ϵ also undergoes a peritectoid decomposition, $\epsilon \rightarrow \zeta+\alpha$.

The ζ phase ($x=1{\cdot}78$) is apparent at all pressures up to 45 torr. At temperatures below that for the equilibrium $\epsilon \rightleftharpoons \zeta+\alpha$ it is in equilibrium with ϵ on the right. Above this temperature the $\zeta+\alpha$ blade rises to a maximum pressure of about 50 torr at a temperature of about 560 °C (see figure 5). At 608 °C ($p \simeq 26$ torr) the peritectoid reaction $\zeta \rightarrow \iota+\alpha$ occurs. ζ therefore reduces to ι on heating at pressures less than 26 torr, and oxidizes to α at higher pressures.

The production of ι from α is not quite as straightforward as that from ζ: it will be considered in the next section.

(ii) *The region* $PrO_{1{\cdot}75}$ *to* σ

For rising temperatures, the break from ι in reduction is sharp, and occurs very close to the ideal ι composition at all pressures below 600 torr: the break temperature decreases with decreasing oxygen pressure. Values of $RT_e \ln p$ for this break vary linearly with temperature; the phase reaction is $\iota \rightarrow \sigma$ across a rising three-phase blade. For pressures greater than 600 torr the break occurs in oxidation (as predicted; Hyde *et al.* 1964). The break temperature *decreases* slightly with *increasing* pressure as required. The only known phase to the right of ι (greater x) in this temperature range is α. The phase reaction is therefore $\iota \rightarrow \alpha$ across a steeply falling blade. (The long almost straight line for the α phase in run 650,

$$460\,^{\circ}\mathrm{C} < t < 780\,^{\circ}\mathrm{C}$$

(see figure 1) can reasonably be extrapolated into that section produced by the oxidation of ι with rising temperature. This is even more obvious in run 715, and supports our contention that it is the α phase that is produced from ι in the reversal.) At a slightly higher temperature the α phase decomposes to σ across a rising $\sigma+\alpha$ blade. The few points for this equilibrium plotted in figure 5 are not in line with those for $\iota+\sigma$ (see especially figure 5 (*b*)). The maximum decomposition temperature of ι is 1054 °C at a pressure of *ca.* 600 torr, and these are taken as the conditions under which the invariant four-phase equilibrium ($\sigma+\iota+\alpha+O_2$) obtains.

Isobaric cooling paths in this region are complex. At pressures below 45 torr the sesquioxide oxidizes directly to ι, with no indication of the σ phase. The oxidation $\sigma \rightarrow \iota$ has already been discussed in detail: $RT_e \ln p$ values for the first break from σ are in line with those for the $\iota \rightarrow \sigma$ conversion on heating.

PHILOSOPHICAL TRANSACTIONS OF THE ROYAL SOCIETY A MATHEMATICAL, PHYSICAL & ENGINEERING SCIENCES

In runs 205 to 380 (cf. figure 4), undecomposed σ^m then oxidizes to α^m at $RT_e \ln p$ values that are consistent with those for $\sigma \rightarrow \alpha$ at the highest pressures (figure 5 (*b*)). As the temperature continues to fall α^m slowly reduces to ι. We assume the microdomain model here also, so that the gradual elimination of α^m with decreasing temperature is analogous to the contraction of σ^m microdomains described in (*b*) above. Figure 4 suggests that at higher pressures α^m fails to revert completely to ι before the reaction $\iota \rightarrow \alpha$ occurs. Consequently the apparent ι composition at the $\iota + \alpha$ boundary is higher than the true value—hence the anomalous points in the $\iota + \alpha$ region of figure 2.

At still higher pressures (runs 440, 515 and 555) it was not possible to distinguish the two breaks, $\sigma \rightarrow \iota$ and $\sigma^m \rightarrow \alpha^m$. The estimated temperatures for the break from σ are in accord with the view that the initial decomposition product is the ι phase. However, it is clear that the reaction $\sigma^m \rightarrow \alpha^m$ also occurs, since the composition attains values markedly higher than those expected for ι. Hence we conclude that the two processes $\sigma \rightarrow \iota$ and $\sigma^m \rightarrow \alpha^m$ occur almost simultaneously over a small temperature interval. The 'rounding off' of the $W-t$ curves here is typical of situations where two reactions occur almost simultaneously. Figure 5 shows that such behaviour is reasonable since the temperature difference between the blades $\sigma^m + \alpha^m$ and $\sigma + \iota$ is quite small in this region (around 1050 °C).

At pressures greater than 610 torr, the break to σ in reduction and from σ in oxidation occurs across the *stable* $\sigma + \alpha$ three-phase blade. This happens above the temperature of the peritectoid decomposition $\iota \rightarrow \sigma + \alpha$.

One further observation fits neatly into the picture of behaviour in this region—the 'kink' which appears in the heating curves at 100 torr and higher pressures (points marked *K* in figure 4, and clearly apparent in the large-scale inset). In these runs ι is produced by the reduction of α on heating. Since α is cubic and ι rhombohedral, the coherent ι nuclei will again occur in four orientations. The situation is exactly analogous to that for $\sigma \rightarrow \iota$ discussed above. We might therefore expect α^m inclusions in the reaction product. $RT_e \ln p$ values for the 'kink' temperatures fall on the line describing the $\sigma^m + \alpha^m$ equilibrium (figure 5*a*). This is clear evidence for the presence of unconverted α in the matrix of ι microdomains. Another result of this incomplete conversion is an apparent ι composition that is again too high. When the sample temperature rises to that of the $\sigma^m + \alpha^m$ blade the unconverted α suddenly decomposes more rapidly (hence the kink), apparently producing ι.

(iii) *The region σ to* $PrO_{1.5}$

On their own, the present data are inadequate for a satisfactory resolution of the phase relations in this region; the values of the partial molar free energy of oxygen ($RT_e \ln p$) are too inaccurate in the relevant range of oxygen pressures (< 10 torr). In addition, there is the complication resulting from the existence of two modifications of the sesquioxide, the *A* and *C* forms (θ and ϕ respectively). It is evident (Warmkessel, Tilley, Bevan, Eyring & Hyde 1964, unpublished) that the initial product in the reduction of PrO_x by dry hydrogen is the topotactically related *C* form. This then transforms *irreversibly* to the *A* form. The rate of transformation increases sharply with increasing temperature, being immeasurably slow below 700 °C and very rapid above 800 °C (cf. Chapin, Finn & Honig 1965). In the isobaric experiments therefore, the behaviour in reduction may be controlled by the existence, or potential existence, of *C*-type $PrO_{1.5}$. However, complete reduction to $PrO_{1.5}$ at measurable oxygen

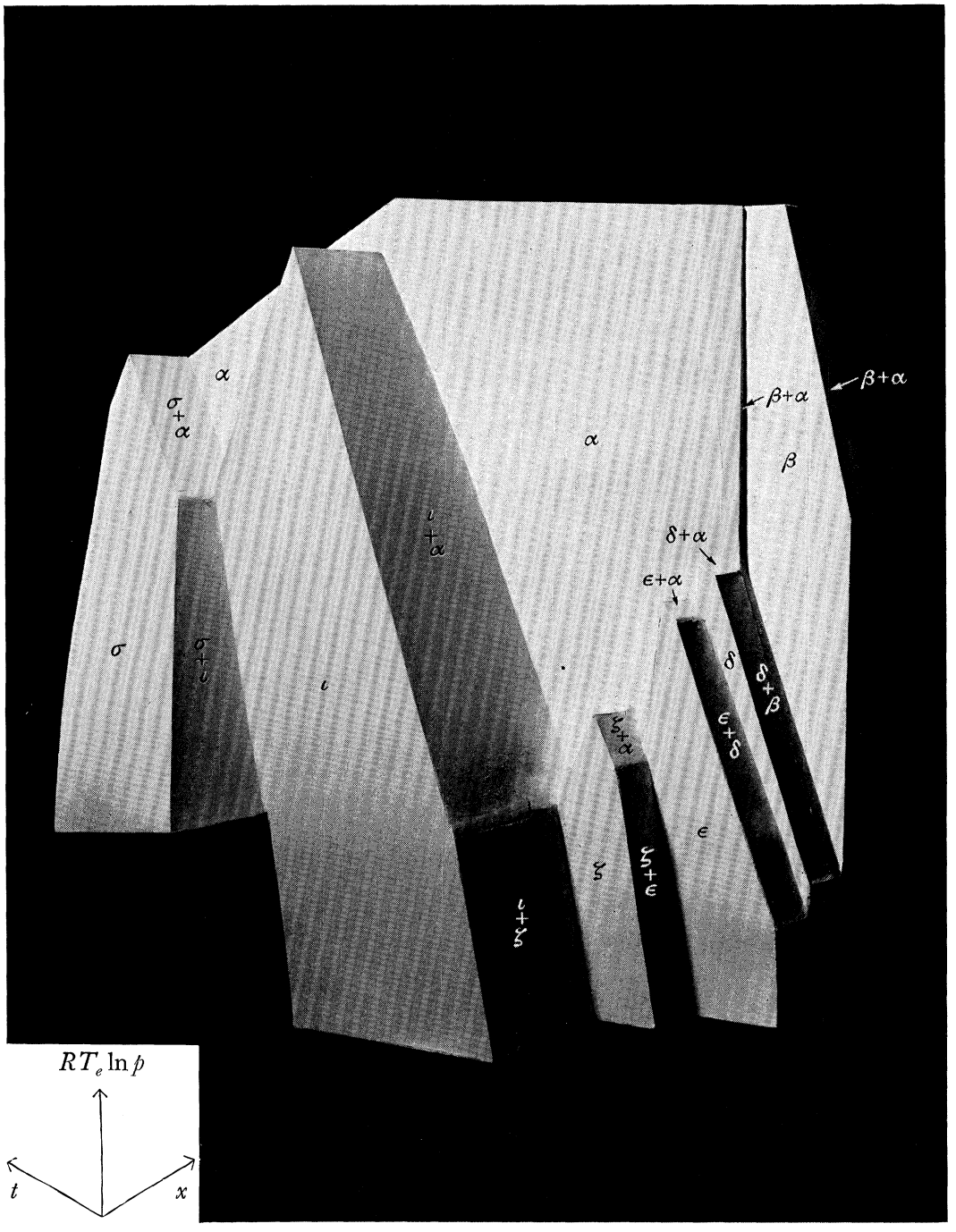

FIGURE 9. Three-dimensional model of the praseodymium oxide + oxygen phase diagram in the composition range $PrO_{1.65}$ to $PrO_{1.84}$: temperature (t)–composition (x)–partial molar free energy of oxygen ($RT_e \ln p$).

(*Facing p.* 602

PHILOSOPHICAL TRANSACTIONS OF THE ROYAL SOCIETY A MATHEMATICAL, PHYSICAL & ENGINEERING SCIENCES

pressures requires high temperatures (above 1000 °C) as the present work shows. Thus, any sesquioxide produced under these conditions may transform to the A modification. Subsequent oxidation would then be controlled by equilibria involving the A form.

Faeth (1961) has examined the isothermal oxidation of A-form sesquioxide, and reports a 'break pressure' defined (Honig *et al.* 1963) as the minimum oxygen pressure, p_c, at which A-type $PrO_{1.5}$ undergoes sudden, rapid oxidation. His data are in good agreement with our own sparse results in this region (runs 0, 1, 3, 10, 19, 35 and 45). The graph of $RT\ln p_c$ against t (figure 5 (b) and (c)) consists of two linear segments intersecting at *ca.* 910 °C and an oxygen pressure of 10 torr. We have previously suggested (Hyde *et al.* 1964) that these data represent excess free energies for the formation of a critical nucleus of the product phase—ι for $t < 910$ °C and σ for $t > 910$ °C. Runs 10 and 45 (figure 1) now substantiate Honig's view (1963, private communication) that they are equilibrium data, and they therefore relate to the equilibria $\theta \rightleftharpoons \iota$ and $\theta \rightleftharpoons \sigma$ respectively. It follows that σ exists *metastably* at temperatures below 910 °C. However, its reversion to the more stable θ would certainly be infinitely slow below 700 °C. There are therefore two sets of phase relationships, depending on whether the transformation $\sigma^m \rightarrow \theta$ occurs slowly or quickly.

On this basis, the isobaric heating path at oxygen pressures less than 10 torr lies on the stable ι surface and continues across that part of it which is metastable with respect to the reaction $\iota \rightarrow \theta$. The metastable equilibrium transition $\iota^m \rightarrow \sigma^m$ then occurs, and σ^m persists until θ nucleates at a much higher temperature. For $p > 10$ torr the path lies on the stable ι surface, crosses the stable $\iota + \sigma$ blade and continues across the σ surface, again into the region σ^m which is metastable with respect to the reaction $\sigma \rightarrow \theta$. The proposed phase relationships, stable and metastable, are shown in figures 2 and 5 (c).

We have observed a break $\sigma \rightarrow PrO_{1.5}$ at very high temperatures and relatively low oxygen pressures. The fact that the left-hand 'phase boundary' of σ (its composition at this break) appears to move *right* with increasing temperature leads us to suspect that this may be a non-equilibrium process, $\sigma^m \rightarrow \theta$: the temperature at which rapid transformation occurs increases with increasing oxygen pressure, as does the limiting composition of σ. The transformation of the fluorite-related σ to the hexagonal A form is difficult because it is 'reconstructive' (Buerger 1951). Our interpretation of the observed behaviour suggests that the conversion $C \rightarrow A(\phi \rightarrow \theta)$ is a monotropic transformation (cf. Roth & Schneider 1960; Warshaw & Roy 1961); that the cubic sesquioxide is a 'compositionally stranded phase' (Buerger 1951). Further work on this problem is in progress. Behaviour corresponding to the equilibrium situation, as described above, *is* observed for the system $CeO_x + O_2$ (Bevan & Kordis 1964).

5. The phase diagram

(a) *Construction*

In reduction, the extrapolated composition at the break temperature is taken to be the left-hand boundary of the decomposing phase at that temperature. In oxidation, points so obtained represent right-hand boundaries. This procedure assumes that the solid is monophasic at the decomposition temperature: exceptions have already been pointed out and discussed. The resulting t-x diagram is virtually complete for the region $1{\cdot}65 < x < 1{\cdot}84$; more data are required before the regions $1{\cdot}5 < x < 1{\cdot}65$ and $1{\cdot}84 < x < 2{\cdot}0$, especially the former, can be described completely.

Finally, the additional information required to define the three dimensional p-x-t relations (shown in figure 9, plate 11) has been derived from figure 5. This comprises the pressure/temperature dependence of the three-phase blades; some idea of the pressure maxima, together with the temperatures at which these occur (i.e. the approximate values of p and t at the summits of the blades); and the various peritectoid and eutectoid pressures and temperatures. These invariant conditions are set out in table 2.

TABLE 2. INVARIANT AXES IN THE PRASEODYMIUM + OXYGEN PHASE DIAGRAM

		oxygen pressure (torr)			temperature (°C)		
equilibrium†	type	'heating' 5(*a*)‡	'cooling' 5(*b*)‡	'average' 5(*c*)‡	'heating' 5(*a*)‡	'cooling' 5(*b*)‡	'average' 5(*c*)‡
$\beta \rightleftharpoons \beta' + \alpha$	peritectoid	$4{\cdot}7 \times 10^4$ (62 atm)	$5{\cdot}1 \times 10^4$ (67 atm)	$5{\cdot}5 \times 10^4$ (73 atm)	488	467	476
$\beta' \rightleftharpoons \beta + \delta$	eutectoid	22_3	21_4	22_8	458	454	456
$\delta \rightleftharpoons \beta + \epsilon$	eutectoid	4·9	7·8	7·6	375	367	378
$\delta \rightleftharpoons \beta' + \epsilon$	peritectoid	12_1	15_0	13_7	476	477	477
$\epsilon \rightleftharpoons \beta' + \zeta$	peritectoid	34	39	38	519	520	519
$\zeta \rightleftharpoons \beta' + \iota$	peritectoid	28	24	26	608	611	608
$\iota \rightleftharpoons \beta' + \sigma$	peritectoid	61_5	55_1	59_2	1053	1051	1054
$\sigma \rightleftharpoons \iota + \theta$	eutectoid	—	10	10	—	906	911
$\delta + \beta' + O_2$	pressure maximum	32_8	32_2	29_9	470	471	469
$\epsilon + \beta' + O_2$	pressure maximum	12_3	15_7	13_7	477	485	477
$\zeta + \beta' + O_2$	pressure maximum	50	53	49	565	556	556
$\iota + \beta' + O_2$	pressure maximum	$1{\cdot}2 \times 10^3$ ($1{\cdot}5_5$ atm)	$1{\cdot}4 \times 10^3$ (1·85 atm)	$1{\cdot}2 \times 10^3$ ($1{\cdot}5_5$ atm)	934	944	939

† β' is α on the left-hand side of the miscibility gap; in the table, α denotes $PrO_{2-\Delta}$, i.e. α on the right-hand side of the miscibility gap.
‡ Figure numbers.

(*b*) *Description and interpretation*

At lower temperatures, in addition to the sesquioxide and dioxide, a sequence of stoichiometric phases obtains in the composition range $1{\cdot}71 < x < 1{\cdot}84$. At higher temperatures these decompose: the peritectoid temperature increases with decreasing oxygen content, so that an increasing composition range is occupied by the non-stoichiometric α phase. Non-stoichiometric σ similarly appears to the left of ι, but no intermediate stoichiometric phases are seen in this region.

The narrow homogeneity ranges of the intermediate phases β, δ, ϵ, ζ and ι suggest that they are highly ordered. An important aspect of the $PrO_x + O_2$ system emerges when one examines their stoichiometries: they appear to constitute an incomplete homologous series whose generic formula is Pr_nO_{2n-2}. Observed values of n are 7, 9, 10, 11, 12, together with 4 and ∞ when C-Pr_2O_3 and PrO_2 are included. Agreement between calculated and measured compositions is very good (see table 3).

The rarity of miscibility gaps with upper consolute points (cf. figure 2) emphasizes the high degree of structural order in the intermediate phases. 'Continuity of state', an inevitable consequence of the earlier models of gross non-stoichiometry (Anderson 1945; Rees

1954; etc.) is replaced by discontinuous order-disorder transitions—the peritectoid decompositions of the intermediate phases. However, the following observations would seem to make it quite clear that neither the order nor the disorder is complete:

(1) The intermediate phases *do* have a small homogeneity range: some disorder therefore persists in the 'ordered' phases (cf. § 1). (At the same time, this would be scarcely detectable by X-ray diffraction. A composition range $\Delta x = 0{\cdot}003$ (cf. table 3) implies a variation of only *ca.* 0·02 % in the lattice parameter; i.e. $\Delta a_0 \simeq 0{\cdot}001$ Å for the pseudofluorite cell.)

TABLE 3. STOICHIOMETRY OF THE KNOWN MEMBERS OF THE PROPOSED HOMOLOGOUS SERIES, Pr_nO_{2n-2}

value of n	stoichiometric formula	x in PrO_x	experimental value of x (this work)	phase symbol
4	Pr_2O_3	1·500	1·500	ϕ
7	Pr_7O_{12}	1·714	1·713 to 1·719	ι
9	Pr_9O_{16}	1·778	1·776 to 1·778	ζ
10	Pr_5O_9	1·800	1·799 to 1·801	ϵ
11	$Pr_{11}O_{20}$	1·818	1·817 to 1·820	δ
12	Pr_6O_{11}	1·833	1·831 to 1·836	β
∞	PrO_2	2·000	—	α

(2) The ordered Pr_nO_{2n-2} phases persist up to quite high temperatures while the disordered α, in the same composition range, extends to much lower temperatures; to a minimum of 456 °C. It is therefore inconsistent to invoke almost perfect ordering of anion vacancies in the one case and complete randomness in the other. To particularize, in the very narrow composition range $1{\cdot}81 < x < 1{\cdot}84$, at 460 °C three phases, δ, α and β, are observed. The first and third are presumed to be highly ordered; it is inconceivable that, at an intermediate composition, the second should be perfectly disordered. The difficulty may be removed simply by allowing substantial ordering of the 'vacancies' within microdomains which are themselves randomly distributed. We therefore assume that in α, and by analogy in σ also, epitaxy between domains of different but related structures replaces, or augments, the simple twinning invoked in § 4 (*b*). This topic will be resumed below (§ 6 (*e*), § 7) after examining the available structural information.

6. COMPARISON WITH OTHER DATA

(*a*) *Pressure-composition isotherms*

We have suggested that much of the new data reported here is close to equilibrium. Comparison with the isothermal equilibrium results of Ferguson *et al.* (1954), Czanderna (1957), and Faeth (1961; see Honig *et al.* 1963) should provide a check on this assumption. To facilitate the comparison we have recalculated the three sets of $(p\text{-}x)_t$ data and plotted them in the form $RT\ln p$ against x. Values of $RT_e\ln p$ for the start of the various phase reactions have been extracted by the extrapolation technique used with the *W-t* isobars (§ 4 (*a*)). They are compared with those from the isobaric study by plotting them on the average graph of $RT_e\ln p$ against t (figure 5 (*c*)) as shown in figure 10. In general, agreement is quite good, especially for Ferguson's data. There is rather poorer agreement with Faeth's results in the region of δ, ϵ and ζ, particularly at lower temperatures where Faeth's points are consistently higher than ours by about 35 degC.

One puzzling feature of Faeth's hysteresis loops is clarified when they are examined in terms of the phase diagram (figure 5 (*c*)). In each of the isotherms 450, 465, 550 and 640 °C (Honig *et al.* 1963) it appears that, for a given loop, the pressure at which oxidation commences is *less* than that at which reduction commences. It is now seen that each of these loops is, in fact, two loops; that an additional phase obtains between those at the ends of the

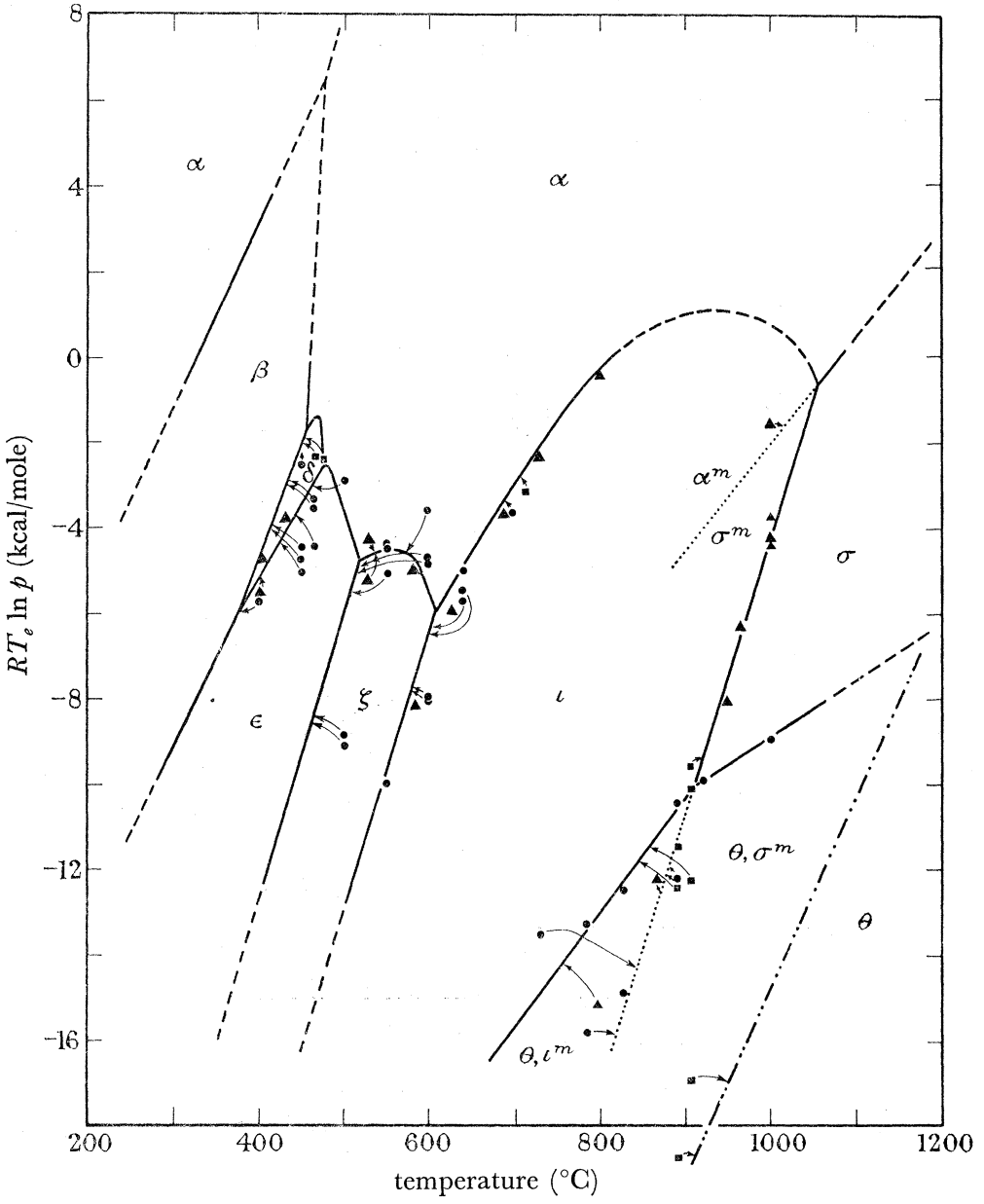

FIGURE 10. Phase 'equilibrium' data from isothermal studies plotted on figure 5 (*c*). ▲, Ferguson *et al.* 1954; ■, Czanderna 1957; ●, Faeth 1961.

loops—δ, δ, ϵ and ζ respectively. In fact, the experimental data (Faeth 1961) show that there are slight breaks in the smooth $(p\text{-}x)_t$ oxidation curves at just the appropriate compositions ($x = 1{\cdot}81_8$, $1{\cdot}81_9$, $1{\cdot}80_0$, $1{\cdot}78_0$ respectively). When this is taken into account there is, in all cases, good agreement between the initial oxidation and reduction pressures for a given reaction.

The outstanding discrepancy between the present work and that of Ferguson *et al.* (1954) appears in their 946, 962 and 998 °C isotherms (figure 11). These strongly suggest a stable phase at $x = 1{\cdot}706$ which, in a previous paper (Hyde *et al.* 1964), we have called the ι' phase.

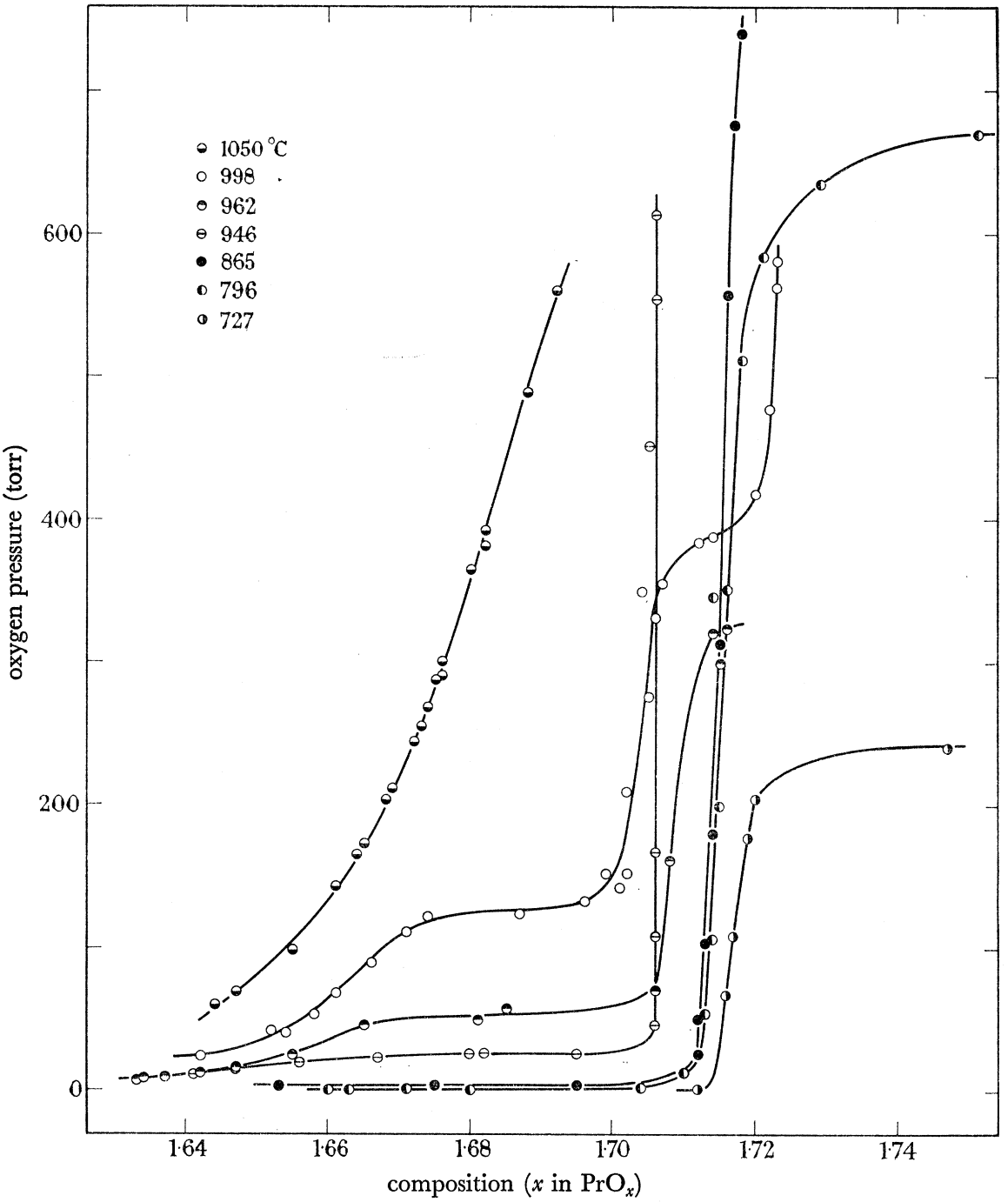

FIGURE 11. Isotherms of Ferguson *et al.* (1954) plotted on an extended composition scale in the range *ca.* $PrO_{1{\cdot}63}$ to $PrO_{1{\cdot}75}$, 727 to 1050 °C, 0 to 760 torr.

Our earlier discussion (§ 4 (*b*)) of the oxidation of σ rejects this interpretation and proposes that the oxidation $\sigma \rightarrow \iota$ is inhibited by the formation of a pseudo-phase. Nevertheless, at the lowest pressures (and temperatures) the oxidation does proceed to completion over a

temperature interval of about 100 degC (runs 45, 60 and 100). At higher pressures and temperatures another process intervenes, $\sigma^m \rightarrow \alpha^m$ (runs 151, 205, 255, 315, 380, 440 and 505). It is of the utmost significance that Ferguson's 998 °C isotherm breaks right, in oxidation, at the calculated pressure for this reaction (see figure 11). We therefore suggest that the isotherms indicate a *pseudo-phase* at $x = 1{\cdot}706$, and are displaced from $x = 1{\cdot}714$ because of incomplete conversion of σ to ι. However, if this is so, we might expect to observe the oxidation $\sigma^m \rightarrow \alpha^m$ in all three isotherms. It is observed at 998 °C; there is indication of a gradual oxidation from $x = 1{\cdot}706$ with increasing oxygen pressure at 962 °C; but the 946 °C isotherm is vertical at $x = 1{\cdot}706$ up to a pressure of 615 torr. This last behaviour emphasizes the stability of the microdomain texture—it is the only vertical isotherm recorded by Ferguson—but it remains somewhat puzzling. Furthermore, the α phase produced at 998 °C is metastable with respect to ι, but the isobars show that at this high temperature the formation of ordered ι from disordered α^m is likely to be slow: it was not observed in the isothermal study.

An abrupt transition in the pattern of Ferguson's isotherms between 946 and 865 °C is apparent in figure 11. It is now clear that this is a consequence of the eutectoid reaction $\sigma \rightarrow \theta + \iota$ at 910 °C. The starting material in the isothermal measurements was always θ (*A*-form sesquioxide produced by evacuating the sample overnight at 1000 °C). Above 910 °C θ oxidizes first to σ and then to ι, this last stage being inhibited. Below 910 °C θ oxidizes directly to ι; σ does not appear; and the product is sufficiently well ordered to have the correct stoichiometry. It is relevant that θ and ι both have a unique trigonal axis and that $\theta \rightarrow \iota$ appears to be an *epitactic* transformation (Mackay 1961) with coherence between the phases and coincidence of the trigonal axes (Eyring & Holmberg 1963; cf. § 6).

(*b*) *Differential thermal analysis*

We have not carried out any differential thermal analysis (d.t.a.) in conjunction with the present isobaric thermal gravimetric analysis. However, the results of such studies on praseodymium oxide at various oxygen pressures (Guth *et al.* 1954), and in 1 atm pressure of either oxygen or nitrogen (Kuntz & Eyring 1959) are available. We have compared the present results with these earlier data: qualitatively, agreement is good; quantitatively it is poor, temperature discrepancies being as much as 100 degC. In view of the excellent agreement between our data and those of Ferguson *et al.*, and the fair agreement with Faeth, we assume the d.t.a. temperatures to be in error (they are all low). This accounts for the discrepancy between the $\beta \rightleftharpoons \beta'$ transformation temperature given above, *ca.* 460 °C, and that given previously, 400° (Hyde *et al.* 1964). The latter was estimated from d.t.a. curves.

The comparison shows that fifteen different phase reactions are involved in the d.t.a. This emphasizes the difficulty of interpreting such data in the absence of other information on the phase relations.

(*c*) *Electrical measurements*

Resistivity measurements have previously been carried out using a sintered pellet of PrO_x powder (Eyring & Baenziger 1962). Three isobars were measured over the temperature range 350 to 850 °C at oxygen pressures of 5×10^{-7}, 1 and 95 torr. It was noted that, apart from a general reduction in resistivity with increasing temperature, there were distinct discontinuities at certain temperatures. While the resistivity changes at these points were

quite small compared with the overall change, they were outside the limit of experimental error, and reproducible. They occurred at temperatures in good agreement with those calculated from figures 5*a* and *b* for the various phase reactions at the same pressures. Similar steps appear when isothermal thermoelectric power values at various oxygen pressures are plotted against the oxide composition, x (Honig *et al.* 1964).

(*d*) *Kinetic studies*

Several studies of the rate of oxidation and reduction of various praseodymium oxides have been carried out in our laboratories (Kuntz & Eyring 1959; Hyde *et al.* 1965; Hyde, Kuntz, Schuldt & Eyring, to be published). Reactions involving phases with $x \geqslant 1{\cdot}714$ have rates that are consistent with a sequence of phase-boundary-controlled reactions. For present purposes the significant results are the compositions of the various phases, as determined from the rate equation for this mechanism. They are slightly temperature- and pressure-dependent, namely $x = 1{\cdot}99$ to $2{\cdot}00$; $1{\cdot}83$ to $1{\cdot}84$; $1{\cdot}795$ to $1{\cdot}805$; $1{\cdot}777$ to $1{\cdot}787$; $1{\cdot}720$. The agreement between these x values and those in table 1 provide substantial mutual support between the two sets of work.

Furthermore, it is now clear that a barely detectable anomaly in the rate plots for the reduction $PrO_{1{\cdot}83} \rightarrow PrO_{1{\cdot}80}$ results from the production of δ in the kinetic runs. The anomaly occurs consistently at $x = 1{\cdot}814$ to $1{\cdot}818$.

(*e*) *X-ray diffraction investigations*

The diffraction data available when these isobaric studies were completed have been summarized by Eyring & Holmberg (1963). They substantiate the present results but are less detailed, showing:

(I) $PrO_{1{\cdot}5}$, types A (hexagonal) and C (cubic); θ and ϕ respectively.
(II) $PrO_{1{\cdot}50}$ to $PrO_{1{\cdot}70}$, a body-centred cubic phase; σ.
(III) $PrO_{1{\cdot}714} = Pr_7O_{12}$, a well-ordered rhombohedral phase; ι.
(IV) $PrO_{1{\cdot}78}$, thought to be rhombohedral; ζ.
(V) $PrO_{1{\cdot}79}$ to $PrO_{1{\cdot}83}$, 'X-ray diffraction patterns show broad lines which are definitely complex'. Additional phases, including $PrO_{1{\cdot}80}$, were believed to exist in this region.
(VI) $PrO_{1{\cdot}833} = Pr_6O_{11}$, thought to have been fluorite-type but, on the basis of some extra, very weak lines, possibly of lower symmetry and/or larger unit cell; β.
(VII) PrO_2, fluorite, stoichiometric at room temperature; α.

Few structures were completely resolved, and it was gradually realized that this state of affairs was at least partly due to the very high oxygen mobility in these oxides. This prevents the quenching-in of composition and order in samples equilibrated at even moderate temperatures. Also, if the annealing temperature is above the peritectoid temperature of a phase in the composition range being studied, then annealing clearly cannot effect ordering in that phase.

The present work defines the previously unknown ambient conditions for the preparation of annealed, well ordered crystalline samples at temperatures sufficiently low for subsequent quenching to be effective: powder-diffraction studies on such samples have since been carried out (Sawyer, Hyde & Eyring 1965). The results confirm the existence of β, δ, ϵ and ζ

as highly ordered superstructures derived from the parent fluorite lattice; each is of low symmetry (triclinic) and narrow homogeneity range. Furthermore, the changes in the various diffraction patterns during annealing are consistent with our notions of micro-domain texture and disordering by successive stages. Thus, the rhombohedral symmetry previously ascribed to $PrO_{1.78}$ (later modified to hexagonal as a result of X-ray diffraction studies on single crystal samples; N. C. Baenziger 1963, private communication) is now thought to be a pseudosymmetry resulting from numerous stacking faults in the triclinic product, due to multiple nucleation.

The earlier work also produced evidence of multiple nucleation and epitaxy in the oxidation of monocrystalline A-$PrO_{1.5}$. The stacking sequence of cation layers ($(000l)$ planes in the hexagonal sesquioxide, (111) planes in fluorite-related PrO_x) is such that two different product orientations are possible:

$$\ldots\ldots\Delta\nabla\Delta\nabla\Delta\nabla\ldots\ldots\rightarrow\ldots\ldots\Delta\Delta\Delta\Delta\Delta\Delta\ldots\ldots,$$

or

$$\ldots\ldots\Delta\nabla\Delta\nabla\Delta\nabla\ldots\ldots\rightarrow\ldots\ldots\nabla\nabla\nabla\nabla\nabla\nabla\ldots\ldots.$$

Single crystal fragments of products ($x = 1{\cdot}71, 1{\cdot}79$) were usually observed to be twinned, $\ldots\Delta\Delta\Delta\nabla\nabla\nabla\ldots$, such stacking faults being most simply explained by multiple coherent nucleation. The product of another oxidation ($x = 1{\cdot}53$) consisted of A-$PrO_{1.5}$ plus Pr_7O_{12}, epitaxially related with coincident trigonal axes, $\ldots\Delta\nabla\Delta\nabla\Delta\Delta\Delta\Delta\Delta\ldots$. It is relevant that the lattice misfit in this case ($(0001) \parallel (111)$) is greater than would be produced by epitaxy, as proposed above, between adjacent Pr_nO_{2n-2} phases (cf. § 5 (b), also § 7 below).

These last cases of disorder differ from those postulated earlier in that they involve the cation lattice. For this reason they are readily observed by X-ray powder diffraction: disorder in the anion lattice is not as easily detected. However, it may be noted that the case of epitaxy also involves the anion lattice. Pr_7O_{12} has one-seventh of the fluorite-type anion sites unoccupied; A-$PrO_{1.5}$ has no anion 'vacancies': there is therefore a vacancy concentration gradient in the sequence of anion planes parallel to, and across, the epitaxial plane.

A final speculation

The postulated homologous series also appears in the related systems TbO_x+O_2, CeO_x+O_2, although fewer members (R_nO_{2n-2}) are known in these cases. Analogous phases in the three systems are believed to have similar or identical structures (Hyde & Eyring 1965).

A logical sequel would be to characterize the structural mechanism whereby the series may be generated from the fluorite parent, but this development is handicapped by the lack of detailed structural knowledge. Crystallographic 'shearing', as observed by Magnéli and co-workers in the various oxides of Mo, W, Ti etc. (see, for example, Wadsley 1964), is ruled out by the absence of short metal–metal distances in the derived lanthanide oxide phases.† We have tentatively proposed a model in which the various structures are produced by ordering anion vacancies into 'strings' parallel to one ($\beta, \delta, \epsilon, \zeta, \iota$) or all four ($\phi$) $\langle 111 \rangle$ directions of the ideal fluorite lattice (Hyde & Eyring 1965). This description is correct for ϕ and almost certainly for ι also: for the other phases it is consistent with their observed

† An exception is the hexagonal A-form sesquioxide, θ. Its structure *is* related to the fluorite-type through shear (Eyring & Holmberg 1963). However, it is not a member of the series proposed here.

PHILOSOPHICAL TRANSACTIONS OF THE ROYAL SOCIETY A MATHEMATICAL, PHYSICAL & ENGINEERING SCIENCES

powder diffraction patterns (Sawyer *et al.* 1965). In a perfect crystal of an intermediate phase the strings would be infinite in length and perfectly ordered. In the solid solution phases, α and σ, they are presumed to be of finite random lengths.

Regarding these latter, it is relevant that the $\sigma+\alpha$ blade persists up to the highest experimental temperatures; 1076 °C in PrO_x+O_2, 1169° C in CeO_x+O_2 (Bevan & Kordis 1964) and 1600 to 1700 °C in analogous ternary systems, $M_2O_3+M'O_2$ (Bevan, Barker, Martin & Parks 1965). In fact, as far as we are aware, there is *no* reliably authenticated case of miscibility between σ and α (cf. Bevan *et al.*). This argues for a radical and very persistent structural difference between them; a state of affairs that is clearly germane to the general problem of non-stoichiometry. These phases have both been regarded as disordered fluorite-derived structures, and understanding is not significantly advanced by observing that α is oxygen-deficient fluorite-type but σ is oxygen-excess *C* type. That non-stoichiometric $\overline{RO}_{1.5}$ and $\overline{RO}_2$ should have such a narrow 'miscibility gap', e.g. $PrO_{1.695}$ to $PrO_{1.725}$, and that it should persist to such high temperatures without closing or even narrowing is rather remarkable. We can only speculate on the nature of the difference, extrapolating from our model of the ordered phases as fluorite-derived structures.

It seems entirely reasonable that σ is simply ϕ with interstitial oxygen; i.e. some of the 'vacancies' are occupied so that the strings are interrupted. However, the arrangement of strings is not thereby affected: the body-centred cubic symmetry of ϕ persists in σ. A model of α is less readily derived; but it would seem logical again to assume finite strings arranged as in the ordered phases in the same composition range, i.e. parallel, so that they are grouped into 'bundles'. Its face-centred *cubic* symmetry shows that these short bundles, if they exist, are distributed over all four possible orientations. This is consistent with the difficulty of ordering apparent in the conversion of α to ι, ζ, ϵ, δ or β, and with the presence of α^m in the product of the reduction $\alpha \rightarrow \iota$ (see § 4 (*b*) and figures 1, 3 and 4). At high 'vacancy' concentrations one could expect 'cross-over' regions occupied by the ends of strings protruding from adjacent bundles oriented in the four possible directions. These micro-regions would have a structure similar to that of σ, and this would, at the same time, explain both (1) the ease of conversion $\alpha \rightleftharpoons \sigma$ (nucleation is clearly no problem in either direction); and (2) the *diffuse C*-type superstructure reflexions observed in powder diffraction diagrams of the face-centred cubic α phase in the analogous ternary systems, when the anion vacancy concentration is greater than *ca.* 10 % (McCullough & Britton 1952; Brauer & Gradinger 1954; Bevan *et al.* 1965).

Irrespective of the merits of this model, partial order in α is consistent with the work of Hoch & Yoon (1965). These authors have pointed out that a random anion-vacancy model for widely non-stoichiometric CeO_x (α phase) is incompatible with its observed behaviour in the range $1{\cdot}8 < x < 2{\cdot}0$. Using an Anderson-type model and the tensimetric data of Brauer *et al.* (1960), they calculated an oxygen-vacancy interaction energy, $E_{vv} = 120$ kcal/mole. From this one deduces a critical temperature $T_c = E_{vv}/2R \simeq 30000$ °K. The observed value, between the low temperature phases $CeO_{1.813}$ and CeO_2 is 958 °K (Brauer & Gingerich 1960). A completely random vacancy distribution would therefore seem to be ruled out (cf. § 5 (*b*)). However, it may also be relevant that, as Cahn (1961) has shown, coherence between two phases may drastically depress the critical temperature—by 2000 °K in the extreme case of AuNi (cf. § 4 (*b*)).

The minimal disorder in the 'ordered' phases Pr_nO_{2n-2} could possibly be due to Frenkel defects in the anion lattice—the interstitial ion being an occupied 'vacancy'. Maximum concentrations of about 0·1 % vacancies and 1 to 2 % interstitials are necessary to explain the observed homogeneity ranges (cf. table 3). These are rather high values, and it seems to us more plausible that this disorder is due, at least partly, to *heterophase fluctuations* (Frenkel 1946); i.e. the line defects are occasionally arranged as in an adjacent ordered phase. This is compatible with the rapid nucleation that occurs in the phase reactions. Hysteresis would then be a consequence of the elastic strain resulting from coherence at heterophase boundaries (cf. Everett & Nordon 1960); and Cahn's theories of coherent fluctuations and spinodal decomposition would seem to be appropriate (see, for example, Cahn 1962). However, the development of a quantitative theoretical treatment on this basis is something for the future.

The line defect proposed here is a one-dimensional analogue of the antiphase boundary (a.p.b.) plane in AuCu. The presence of ordered a.p.b. planes in AuCu II, and disordered a.p.b. planes in AuCu I; and the microdomain twinning produced in the transformation AuCu I → AuCu II are well documented by direct observation in the electron microscope (Pashley 1964). This *observed* behaviour has much in common with our proposed explanations for $PrO_x + O_2$.

8. Conclusions

Isobaric thermo-gravimetric analysis is revealed to be a powerful method for resolving the behaviour of a sufficiently mobile non-stoichiometric system. It is superior to the more usual isothermal tensimetric method, at least in the case of $PrO_x + O_2$. The amount of detail observed emphasizes that the phase analysis of a complex system demands the acquisition of a large amount of sufficiently accurate data: the present technique makes this task relatively easy.

The results establish:

I. A new homologous series of oxides.

II. The presence, *at equilibrium*, of a small homogeneity range for each of the highly ordered intermediate phases. This implies a minimal amount of disorder which is too small to be detected by less accurate gravimetric or crystallographic studies.

III. The *equilibrium* existence of widely non-stoichiometric phases, even at quite low temperatures.

IV. The appearance of pseudo-phases in reactions attended by an increase in structural order.

They also confirm:

V. Hysteresis in phase transformations.

These, and other quoted observations, expose the inadequacy of the earlier concepts of random point defects in describing grossly non-stoichiometric systems. In contrast, application of a simple microdomain model is successful.

We are grateful for the award of a Fulbright Travelling Fellowship (to D.J.M.B.); for financial support from the United States Atomic Energy Commission and, during the final preparation of the paper, from the Air Force Office of Scientific Research, Office of Aerospace Research, United States Air Force, under A.F.O.S.R. Grant number AF-AFOSR-853-65.

PHILOSOPHICAL TRANSACTIONS OF THE ROYAL SOCIETY A MATHEMATICAL, PHYSICAL & ENGINEERING SCIENCES

References

Anderson, J. S. 1945 *Proc. Roy. Soc.* A, **185**, 69.
Anderson, J. S. 1963 *Adv. Chem. Ser.* **39**, 1.
Anderson, J. S. 1964 *Proc. Chem. Soc.* p. 166.
Anderson, J. S. & Sterns, M. 1959 *J. Inorg. Nucl. Chem.* **11**, 272.
Andersson, S. 1960 *Acta Chem. Scand.* **14**, 1161.
Andersson, S., Collén, B., Kuylenstierna, U. & Magnéli, A. 1957 *Acta Chem. Scand.* **11**, 1641.
Ariya, S. M. & Popov, Yu. G. 1962 *J. Gen. Chem., Moscow*, **32**, 2077
Baenziger, N. C., Eick, H. A., Schuldt, H. S. & Eyring, L. 1961 *J. Amer. Chem. Soc.* **83**, 2219.
Bevan, D. J. M. 1955 *J. Inorg. Nucl. Chem.* **1**, 49.
Bevan, D. J. M., Barker, W. W., Martin, R. L. & Parks, T. C. 1965 *Rare earth research*, vol. 3 (ed. L. Eyring). New York: Gordon and Breach.
Bevan, D. J. M. & Kordis, J. 1964 *J. Inorg. Nucl. Chem.* **26**, 1509.
Bragg, W. L. 1940 *Proc. Phys. Soc.* **52**, 195.
Brauer, G. & Gingerich, K. 1957 *Angew. Chem.* **69**, 480.
Brauer, G. & Gingerich, K. A. 1960 *J. Inorg. Nucl. Chem.* **16**, 87.
Brauer, G., Gingerich, K. A. & Holtschmidt, U. 1960 *J. Inorg. Nucl. Chem.* **16**, 77.
Brauer, G. & Gradinger, H. 1954 *Z. anorg. Chem.* **277**, 89.
Buerger, M. J. 1951 *Phase transformations in solids* (ed. Smoluchowski *et al.*), pp. 183 to 209. London: Chapman and Hall.
Cahn, J. W. 1961 *Acta Metall.* **9**, 795.
Cahn, J. W. 1962 *Acta Metall.* **10**, 907.
Chapin, D. S., Finn, M. C. & Honig, J. M. 1965 *Rare earth research*, vol. 3 (ed. L. Eyring). New York: Gordon and Breach.
Czanderna, A. W. 1957 Thesis, Purdue University.
Everett, D. H. & Nordon, P. 1960 *Proc. Roy. Soc.* A, **259**, 341.
Eyring, L. & Baenziger, N. C. 1962 *J. Appl. Phys.* (Suppl.), **33**, 428.
Eyring, L. & Holmberg, B. 1963 *Adv. Chem. Ser.* **39**, 46.
Faeth, P. A. 1961 Thesis, Purdue University.
Faeth, P. A. & Clifford, A. F. 1963 *J. Phys. Chem.* **67**, 1453.
Ferguson, R. E., Guth, E. D. & Eyring, L. 1954 *J. Amer. Chem. Soc.* **76**, 3890.
Fert, A. 1962 *Bull. Soc. franç. Miner. Cryst.* **85**, 267.
Frenkel, J. 1946 *Kinetic theory of liquids*. Oxford: Clarendon Press.
Gadó, P. 1963 *Acta Cryst.* **16**, A 182.
Guth, E. D. & Eyring, L. 1954 *J. Amer. Chem. Soc.* **76**, 5242.
Guth, E. D., Holden, J. R., Baenziger, N. C. & Eyring, L. 1954 *J. Amer. Chem. Soc.* **76**, 5239.
Guttman, L. 1956 *Solid St. Phys.* **3**, 146.
Hoch, M. & Yoon, H. S. 1965 *Rare earth research*, vol. 3 (ed. L. Eyring). New York: Gordon and Breach.
Honig, J. M., Cella, A. A. & Cornwell, J. C. 1964 *Rare earth research*, vol. 2 (ed. K. Vorres). New York: Gordon and Breach.
Honig, J. M., Clifford, A. F. & Faeth, P. A. 1963 *Inorg. Chem.* **2**, 791.
Hyde, B. G., Bevan, D. J. M. & Eyring, L. 1964 *Rare earth research*, vol. 2 (ed. K. Vorres). New York: Gordon and Breach.
Hyde, B. G., Garver, E. E., Kuntz, U. E. & Eyring, L. 1965 *J. Phys. Chem.* **69**, 1667.
Hyde, B. G. & Eyring, L. 1965 *Rare earth research*, vol. 3 (ed. L. Eyring). New York: Gordon and Breach.
Katz, T. 1950 *Ann. Chim.* (xii), **5**, 5.
Kuntz, U. E. & Eyring, L. 1959 *Kinetics of high-temperature processes* (ed. W. D. Kingery). London Chapman and Hall.

PHILOSOPHICAL TRANSACTIONS OF THE ROYAL SOCIETY A MATHEMATICAL, PHYSICAL & ENGINEERING SCIENCES

Mackay, A. L. 1961 *Reactivity of solids* (ed. J. H. de Boer). Amsterdam: Elsevier.
McCullough, J. D. & Britton, J. D. 1952 *J. Amer. Chem. Soc.* **74**, 5225.
Pagel, H. A. & Brinton, P. H. 1929 *J. Amer. Chem. Soc.* **51**, 42.
Pashley, D. W. 1964 *Modern developments in electron microscopy* (ed. B. M. Siegel). New York: Academic Press.
Pauling, L. & Shapell, M. D. 1930 *Z. Kristallogr.* A, **75**, 128.
Rees, A. L. G. 1954 *Chemistry of the defect solid state.* London: Methuen.
Roth, R. S. & Schneider, S. J. 1960 *J. Res. Natl. Bur. Std.* A, **64**, 309.
Roth, W. L. 1960 *Acta Cryst.* **13**, 140.
Sawyer, J. O., Hyde, B. G. & Eyring, L. 1965 *Bull. Soc. chim. Fr.* p. 1190.
Schuldt, H. S. 1957 Thesis, State University of Iowa.
Sieglaff, C. L. & Eyring, L. 1957 *J. Amer. Chem. Soc.* **79**, 3024.
Simon, W. & Eyring, L. 1954 *J. Amer. Chem. Soc.* **76**, 5872.
Wadsley, A. D. 1964 *Non-stoichiometric compounds* (ed. L. Mandelcorn). London: Academic Press.
Wagner, C. & Schottky, W. 1930 *Z. phys. Chem.* B, **11**, 163.
Warshaw, I. & Roy, R. 1961 *J. Phys. Chem.* **65**, 2048.
Willis, B. T. M. 1963 *U.K.A.E.A. Report*, A.E.R.E.–R 4487.

PHILOSOPHICAL TRANSACTIONS OF THE ROYAL SOCIETY A MATHEMATICAL, PHYSICAL & ENGINEERING SCIENCES

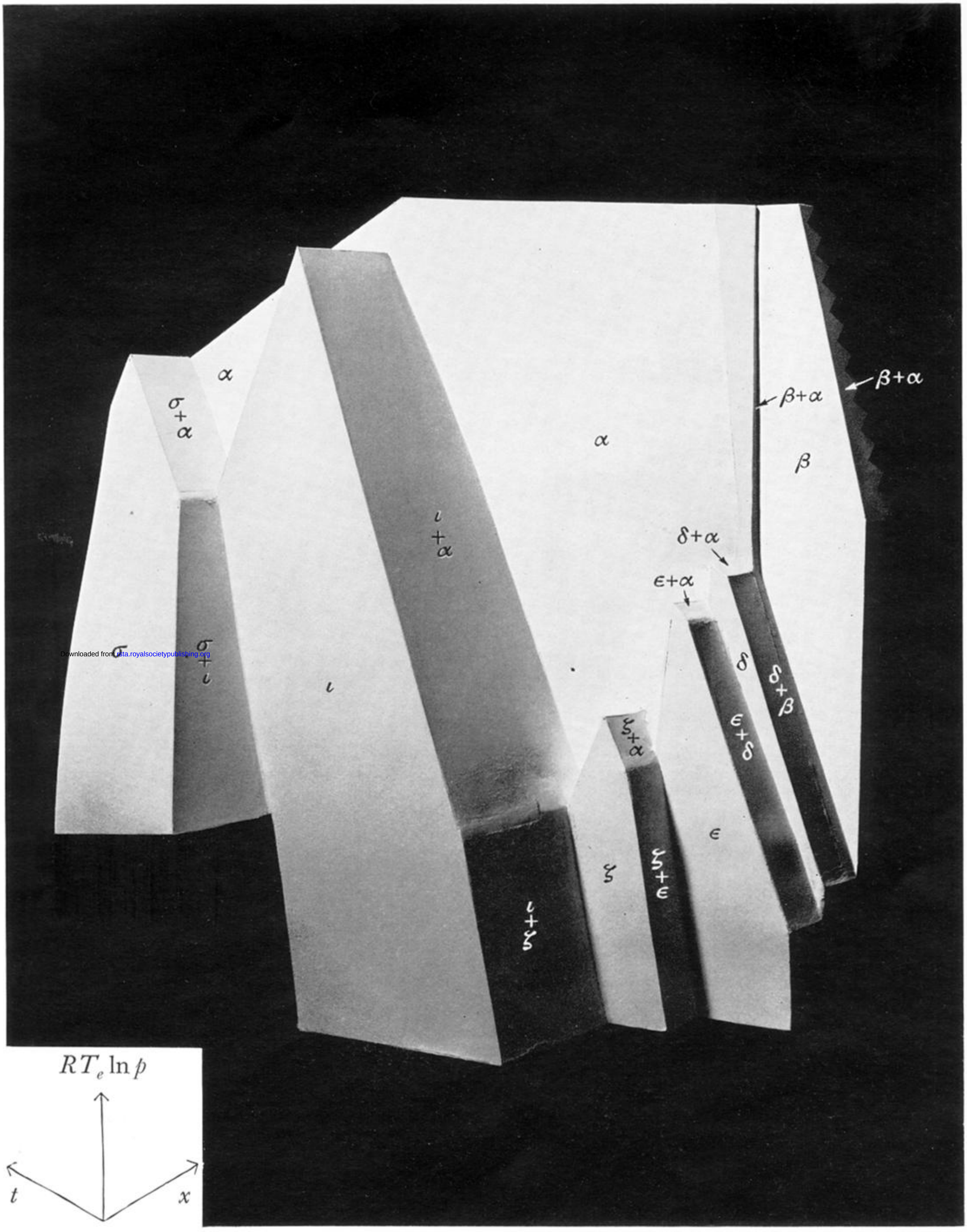

FIGURE 9. Three-dimensional model of the praseodymium oxide + oxygen phase diagram in the composition range $PrO_{1\cdot65}$ to $PrO_{1\cdot84}$: temperature (t)–composition (x)–partial molar free energy of oxygen ($RT_e \ln p$).